Manuscript bioRxiv preprint doi: https://doi.org/10.1101/273722; this version posted March 1, 2018. The copyright holder for this preprint (which was not certified by peer review) is the author/funder. All rights reserved. No reuse allowed without permission. Click here to download Manuscript GSP2Paper V39.docx

1
2
3
4
5
6
7
8
9
10 The conserved phosphatase GSP-2/PP1 promotes germline immortality via
11 small RNA-mediated genome silencing during meiosis
12
13
14
15
16 Katherine Kretovich Billmyre[1,2], Anna-Lisa Doebley[2,7,8], Bree Heestand[1,2], Tony
17 Belicard[3,4], Aya Sato-Carlton[5], Stephane Flibotte[6], Matt Simon[1,2,9], Megan Gnazzo[7],
18 Ahna Skop[7], Donald Moerman[6], Peter Mark Carlton[5], Peter Sarkies[3,4] and Shawn
19 Ahmed[1,2]
20
21
22
23 [1]Department of Genetics, University of North Carolina, Chapel Hill, NC, 27599 USA
24 [2]Department of Biology, University of North Carolina, Chapel Hill, NC, 27599 USA
25 [3]Medical Research Council London Institute of Medical Sciences, Du Cane Road, London, W12
26 0NN, UK
27 [4]Institute for Clinical Sciences, Imperial College London, Du Cane Road, London, W12 0NN, UK
28 [5]Graduate school of Biostudies, Kyoto University, Kyoto, 606-8501, Japan,
29 [6]Department of Zoology, University of British Columbia, Vancouver, British Columbia, Canada
30 [7]Department of Genetics, University of Wisconsin-Madison, Madison, WI 53706
31 [8]Present address: Department of Opthamology, University of Washington, Seattle, WA, USA
32 [9]Present address: Department of Biology, University of Rochester, Rochester, NY, USA
33
34 [*]To whom correspondence should be addressed. E-mail: shawn@med.unc.edu
35
36
37
38

bioRxiv preprint doi: https://doi.org/10.1101/273722; this version posted March 1, 2018. The copyright holder for this preprint (which was not certified by peer review) is the author/funder. All rights reserved. No reuse allowed without permission.

39 **Abstract**

40 Genomic silencing can promote germ cell immortality, or transgenerational maintenance
41 of the germ line, via mechanisms that may occur during mitosis or meiosis. Here we
42 report that the *gsp-2* PP1/Glc7 phosphatase promotes germ cell immortality. We
43 identified a separation-of-function allele of *C. elegans* GSP-2 that caused a meiosis-
44 specific chromosome segregation defect and defects in transgenerational small RNA-
45 induced genome silencing. GSP-2 is recruited to meiotic chromosomes by LAB-1, which
46 also promoted germ cell immortality. Sterile *gsp-2* and *lab-1* mutant adults displayed
47 germline degeneration, univalents and histone phosphorylation defects in oocytes,
48 similar to small RNA genome silencing mutants. Epistasis and RNA analysis suggested
49 that GSP-2 functions downstream of small RNAs. We conclude that a meiosis-specific
50 function of GSP-2/LAB-1 ties small RNA-mediated silencing of the epigenome to germ
51 cell immortality. Given that hemizygous genetic elements can drive transgenerational
52 epigenomic silencing, and given that LAB-1 promotes pairing of homologous
53 chromosomes and localizes to the interface between homologous chromosomes during
54 pachytene, we suggest that discontinuities at this interface could promote nuclear
55 silencing in a manner that depends on GSP-2.

56

57 **Author Summary**

58 The germ line of an organism is considered immortal in its capacity to give rise to an
59 unlimited number of future generations. To protect the integrity of the germ line,
60 mechanisms act to suppress the accumulation of transgenerational damage to the
61 genome or epigenome. Loss of germ cell immortality can result from mutations that

bioRxiv preprint doi: https://doi.org/10.1101/273722; this version posted March 1, 2018. The copyright holder for this preprint (which was not certified by peer review) is the author/funder. All rights reserved. No reuse allowed without permission.

62 disrupt the small RNA-mediated silencing pathway that helps to protect the integrity of
63 the epigenome. Here we report for the first time that the *C. elegans* protein phosphatase
64 GSP-2 that promotes core chromosome biology functions during meiosis is also
65 required for germ cell immortality. Specifically, we identified a partial loss of function
66 allele of *gsp-2* that exhibits defects in meiotic chromosome segregation and is also
67 dysfunctional for transgenerational small RNA-mediated genome silencing. Our results
68 are consistent with a known role of *Drosophila* Protein Phosphatase 1 in
69 heterochromatin silencing, and point to a meiotic phosphatase function that is relevant
70 to germ cell immortality, conceivably related to its roles in chromosome pairing or sister
71 chromatid cohesion.
72
73 **Introduction**

74 Animals, including humans, are comprised of two broad cell types: somatic cells
75 and germ cells. Somatic cells consist of many diverse differentiated cell types, while
76 germ cells are specialized to produce the next generation of offspring. An important
77 difference between these two cell types is that somatic cells undergo aging phenomena
78 while the germ line is effectively immortal and capable of creating new "young" offspring
79 [1]. Understanding the basis of immortality in germ cells may provide insight into why
80 organisms age.

81 In *C. elegans*, disruption of pathways that promote germ cell immortality results
82 in initially fertile animals that become sterile after reproduction for a number of
83 generations. Many such *mortal germline* (*mrt*) mutant strains are temperature-sensitive,
84 becoming sterile at 25°C but remaining fertile indefinitely at 20°C [2]. Mutations that

bioRxiv preprint doi: https://doi.org/10.1101/273722; this version posted March 1, 2018. The copyright holder for this preprint (which was not certified by peer review) is the author/funder. All rights reserved. No reuse allowed without permission.

85 cause a Mrt phenotype have been reported in two distinct pathways: telomerase-
86 mediated telomere maintenance [3,4] and small RNA-mediated nuclear silencing [5–9].
87 Mutations in the PIWI Argonaute protein cause immediate sterility in many species.
88 However, disruption of the *C. elegans* Piwi orthologue PRG-1, which interacts with
89 thousands of piRNAs to promote silencing of some genes and many transposons in
90 germ cells, results in temperature-sensitive reductions in fertility and in an unconditional
91 Mrt phenotype [6–12]. Multiple members of a nuclear RNA interference (RNAi) pathway
92 that promotes maintenance of transgene silencing also promote germ cell immortality
93 and likely function downstream of PRG-1/piRNAs [10,13]. One nuclear RNAi defective
94 mutant, *nrde-2,* a number of heritable RNAi mutants, including *hrde-1*, and two RNAi
95 defective mutants, *rsd-2* and *rsd-6*, only become sterile after growth for multiple
96 generations at the restrictive temperature of 25°C [10,12–16]. These 'small RNA-
97 mediated genome silencing' genes repress deleterious genomic elements via a small
98 RNA-mediated memory of 'self' vs 'non-self' segments of the genome [13,17,18]. The
99 transgenerational fertility defects of such mutants could reflect a progressive desilencing
100 of heterochromatin due to changes in histone modifications downstream of small RNAs,
101 which is modulated by histone modifications that occur in response to small RNAs, such
102 as H3K4 demethylation and H3K9me2/3 [15,19].
103 Pioneering studies in *Neurospora* demonstrated that unsuccessful pairing of DNA
104 during meiotic prophase can trigger small RNA-mediated genome silencing [20], and
105 multigenerational silencing of hemizygous transgenes [21] suggests similar
106 mechanisms may operate in *C. elegans*. Components of the *C. elegans* small RNA-
107 mediated genome silencing machinery, such as the HRDE-1 and PRG-1 Argonaute

bioRxiv preprint doi: https://doi.org/10.1101/273722; this version posted March 1, 2018. The copyright holder for this preprint (which was not certified by peer review) is the author/funder. All rights reserved. No reuse allowed without permission.

108 proteins, are expressed throughout germ cell development [6,10,13,18]. RSD-2 displays
109 a cytoplasmic localization in embryos but becomes a nuclear protein in adults [12],
110 suggesting that aspects of small RNA-mediated genome silencing may be
111 developmentally plastic.

112 Here we report the identification of a hypomorphic allele of *gsp-2*, a PP1/Glc7
113 phosphatase, which fails to maintain germline immortality at 25°C. GSP-2 is one of four
114 PP1 catalytic subunits in *C. elegans* [22,23]. The PP1 phosphatase has roles in many
115 cellular processes including mitosis, meiosis, apoptosis and protein synthesis [24].
116 Previously, GSP-2 has been shown to promote meiotic chromosome cohesion by
117 restricting the activity of the Aurora B kinase ortholog AIR-2 to the short arms of *C.*
118 *elegans* chromosomes during Meiosis I [25,26]. Here, we demonstrate that GSP-2
119 promotes germline immortality via a small RNA-mediated genome silencing pathway,
120 implicating pairing and/or cohesion of meiotic chromosomes in genomic silencing.
121

122 Results

123 Identification of GSP-2 as a temperature-sensitive *mrt* mutant

124 In a screen for *mrt* mutants [2], one mutation that displayed a Temperature-
125 sensitive defect in germ cell immortality, *yp14*, was tightly linked to an X chromosome
126 segregation defect manifesting as a High Incidence of Males (Him) phenotype, such
127 that 3.9% of *yp14* self-progeny were XO males, which significantly greater than the
128 0.05% male self-progeny observed in wildtype animals (Fig. 1A, $p<.0001$). The *yp14*
129 mutation was mapped to Chromosome *III*, and whole genome sequencing revealed
130 missense mutations in 6 genes within the *yp14* interval (Fig. S1A,B). Three-factor

bioRxiv preprint doi: https://doi.org/10.1101/273722; this version posted March 1, 2018. The copyright holder for this preprint (which was not certified by peer review) is the author/funder. All rights reserved. No reuse allowed without permission.

131 mapping of the *yp14* Him and Mrt phenotypes suggested that *yp14* might correspond to
132 the missense mutation in *gsp-2* (Fig. 1C,D) or to a mutation in the G-protein coupled
133 receptor gene *srb-11* (Fig. S1A,B).

134 To test whether the meiotic segregation phenotype of *yp14* was due to a
135 mutation in *gsp-2*, we performed a non-complementation test with a deletion mutation in
136 *gsp-2*, *tm301*. *yp14 / tm301* F1 heterozygous hermaphrodites gave rise to F2 male
137 progeny at a frequency of 5.7% at 20°C, similar to the 3.8% male phenotype observed
138 for *yp14* homozygotes (Fig. S1C). Thus, *tm301* failed to complement *gsp-2(yp14)* for its
139 Him phenotype. In contrast, *gsp-2(tm301) / +* animals did not display a Him phenotype
140 (Fig. S1C). *gsp-2(yp14)* strains also displayed 6% embryonic lethality at 20°C (Fig. 1B).
141 Given that most forms of aneuploidy for the five *C. elegans* autosomes elicit embryonic
142 lethality [27], the simplest explanation for the Him and Embryonic Lethal phenotypes of
143 *gsp-2(yp14)* is that they are due to chromosome mis-segregation. Both of these
144 phenotypes were exacerbated at 25°C (Fig. 1A,B), suggesting that *gsp-2(yp14)* has a
145 chromosome segregation defect that may be mechanistically linked to its Mortal
146 Germline phenotype (Fig. 1A,E). At both temperatures, the X chromosome non-
147 disjunction defect was more pronounced than the embryonic lethality associated with
148 non-disjunction of any of the five *C. elegans* autosomes (Table S1).

149 *gsp-2(tm301)* null mutants immediately exhibited high levels of embryonic
150 lethality at 20°C with a few F3 embryos that survive until adulthood (Fig. 1C), consistent
151 with roles for PP1 in chromosome condensation and segregation during mitosis in
152 several species [28–30]. Mutations that cause chromosome non-disjunction during
153 mitosis occasionally lead to loss of an X chromosome during germ cell development,

bioRxiv preprint doi: https://doi.org/10.1101/273722; this version posted March 1, 2018. The copyright holder for this preprint (which was not certified by peer review) is the author/funder. All rights reserved. No reuse allowed without permission.

154 which could result in the stochastic appearance of XX hermaphrodites with high
155 numbers of XO male progeny [27]. However, jackpots of XO males did not occur when
156 *yp14* mutant hermaphrodites were isolated as single L4 larvae (Fig. 1G), implying that
157 *yp14* is a separation-of-function mutation that specifically compromises the meiotic
158 chromosome segregation function of GSP-2 without affecting its function in mitosis.
159

160 **GSP-2 promotes germline immortality at high temperature**

161 GSP-2 is assumed to be localized to the long arms of meiotic chromosomes
162 through binding to LAB-1, where it antagonizes AIR-2 (Aurora-B kinase) activity to
163 regulate cohesion during meiotic prophase and Meiosis I [26,28,30]. In addition, LAB-1
164 is also present on mitotic chromosomes where it likely antagonizes AIR-2 activity [25].
165 In meiosis, LAB-1 fulfills the roles played by Shugoshin and Protein Phosphatase 2A in
166 many other organisms, by protecting meiotic chromosome cohesion on the long arms in
167 Meiosis I [25,31,32]. Once recruited by LAB-1, GSP-2 keeps REC-8, a meiosis-specific
168 cohesin subunit, dephosphorylated to protect it from premature degradation and
169 chromatid separation [25,26].

170 At 20°C, *gsp-2(yp14)* mutants remain fertile indefinitely, but at 25°C they exhibit
171 sterility between generations F5 and F17 (Fig. 1E,F). We asked if a meiotic function of
172 GSP-2 is relevant to germ cell immortality by first outcrossing a *lab-1* deletion with
173 wildtype and re-isolating *lab-1* homozygotes in an effort to eliminate epigenetic defects
174 that could have accumulated in the parental *lab-1* strain. Outcrossed *lab-1* mutants
175 displayed a Mortal Germline phenotype at 25°C (Fig. 1E,F). We created *lab-1;gsp-2*
176 double mutants, which remained fertile indefinitely when grown at 20°C but displayed a

bioRxiv preprint doi: https://doi.org/10.1101/273722; this version posted March 1, 2018. The copyright holder for this preprint (which was not certified by peer review) is the author/funder. All rights reserved. No reuse allowed without permission.

177 slightly accelerated number of generations to sterility at 25°C in comparison with *lab-1*
178 mutants (Fig. 1E,F). Together, these results suggest that a meiotic function of GSP-2
179 that is directed by LAB-1 promotes germ cell immortality. Moreover, the weak Mortal
180 Germline phenotype of *lab-1* single mutants at 20°C was suppressed by *gsp-2(yp14)*
181 (Log Rank Test, p=.001).
182
183 ***gsp-2* and *lab-1* mutants display common germline defects at sterility**
184 To investigate the cellular cause of transgenerational sterility in *gsp-2(yp14)* and
185 *lab-1* mutants, we examined germline development in animals that became sterile after
186 multiple generations. We previously reported that sterile *rsd-2* and *rsd-6* animals display
187 a wide range of germline sizes, including many with few or no germ cells [12].
188 Interestingly, at the L4 larval stage, we found no significant difference between the
189 germline profiles of *rsd-6* mutants at the generation of sterility and wild-type controls
190 (Fig. 2H, Table S3). Most sterile generation L4 *gsp-2(yp14)* and *lab-1* mutant germlines
191 were normal in size, though a small minority had a reduction in total germline length,
192 resulting in a weak but significant difference in germline profile compared to wild-type
193 (Fig. 2H, Table S3). Differentiating germ cell nuclei in spermatogenesis were observed
194 for sterile generation L4 larvae for all strains (Fig. 2A,H). However, the germlines of two-
195 day-old sterile *gsp-2*, *lab-1* and *rsd-6* mutant adults ranged in size from normal to a
196 complete loss of germ cells (Fig. 2B-E,H), resulting in a strong significant difference
197 when compared to wild-type controls (Table S3 p<1E-80). Given the similarities
198 between the RNAi defective mutant *rsd-6* and *gsp-2*, we studied two additional small
199 RNA silencing mutants. The germline profiles of adult sterile-generation *hrde-1* and

bioRxiv preprint doi: https://doi.org/10.1101/273722; this version posted March 1, 2018. The copyright holder for this preprint (which was not certified by peer review) is the author/funder. All rights reserved. No reuse allowed without permission.

200 *nrde-2* were similar to sterile *gsp-2(yp14)* animals (Fig. 2H, Table S2). Similar to *gsp-2*
201 and *lab-1* mutants, *hrde-1* or *nrde-2* mutant L4 larvae that were poised to become
202 sterile displayed predominantly normal-sized germlines (Fig. 2H). We previously
203 showed that mutations in the cell death genes *ced-3* and *ced-4* partially rescued the
204 empty and atrophy phenotypes observed for germlines of *rsd-2* and *rsd-6* small RNA
205 silencing mutant adults [12], suggesting that apoptosis promotes germ cell atrophy as
206 these animals develop from L4 larvae into adults.
207
208 **Acute loss of GSP-2 does not cause small RNA mutant germline phenotypes**
209 Previous work on GSP-2 in *C. elegans* reported that offspring of *gsp-2(tm301)* F2
210 homozygotes exhibited 98% embryonic lethality and that sterility occurred for F3
211 escapers [28,30]. To determine if acute loss of GSP-2 causes germline atrophy, we
212 examined *gsp-2(tm301)* null mutants grown at 20°C and 25°C. We observed high levels
213 of embryonic lethality for F3 embryos (97%), with a few escapers surviving to become
214 uniformly sterile F3 adults that produced no F4 progeny [28] (Fig. 1B). These very high
215 levels of embryonic lethality contrast with 41.6% embryonic lethality seen in *gsp2(yp14)*
216 F8 animals grown at 25°C (Fig. 1B). *gsp2(tm301)* homozygous F2 animals and their few
217 surviving F3 progeny showed normal germlines, with no morphological defects in
218 germline size or development for either L4 larvae or young adults, which significantly
219 differed from the germline profiles of *gsp-2(yp-14)* animals (Table S2, S3). Therefore,
220 the late-generation sterility phenotype of *yp14* mutants is distinct from the fertility
221 defects that occur in response to acute loss of GSP-2 in maternally depleted F3 deletion
222 homozygotes.

bioRxiv preprint doi: https://doi.org/10.1101/273722; this version posted March 1, 2018. The copyright holder for this preprint (which was not certified by peer review) is the author/funder. All rights reserved. No reuse allowed without permission.

223

224 **A meiotic recombination defect occurs at the generation of sterility**

225 Mature *C. elegans* oocytes typically contain 6 bivalents (pairs of homologous
226 chromosomes held together by crossovers), which can be scored as DAPI-stained
227 bodies. Defects in meiosis can lead to the presence of univalents, which are observed
228 as greater than 6 DAPI bodies per oocyte. We previously observed that small RNA
229 nuclear silencing *mrt* mutants *rsd-2* and *rsd-6* displayed increased levels of univalents
230 at sterility, which were not observed in either wildtype or in fertile *rsd-2* or *rsd-6* mutant
231 late-generation animals grown at 25°C [12]. We measured the presence of univalents in
232 *gsp-2(yp14)* and RNAi mutant strains and found that oocytes of control N2 wildtype or
233 fertile *gsp-2(yp14)* worms grown at 20°C and 25°C almost always contained 6 DAPI
234 bodies representing the 6 paired chromosomes (5 bodies are occasionally scored when
235 bivalents that overlap spatially cannot be distinguished). However, when *gsp-2(yp14)*
236 worms were passaged at 25°C until sterility, only 60% of oocytes containing 6 paired
237 chromosomes with the other 40% containing 7 to 12 DAPI bodies (Fig. 2I). This
238 increase in oocyte univalents was not present in fertile *gsp-2(yp14)* worms, even for
239 late-generation 25°C strains close to sterility (Fig. 2I). We found no univalents in the null
240 *gsp-2* allele *tm301*, either for F2 animals or for rare F3 escapers, consistent with
241 previous observations [28,30]. Together these results emphasize that the germline
242 phenotypes of sterile late-generation *gsp-2(yp14)* animals are distinct from those
243 caused by acute zygotic or maternal loss of GSP-2 [25,26].

244 Given that LAB-1 and GSP-2 promote meiotic chromosome cohesion, we tested
245 the hypothesis that dysfunction of other factors that promote meiotic chromosome

bioRxiv preprint doi: https://doi.org/10.1101/273722; this version posted March 1, 2018. The copyright holder for this preprint (which was not certified by peer review) is the author/funder. All rights reserved. No reuse allowed without permission.

246 cohesion might be sufficient to elicit germline atrophy. Sterile adults of mutant strains
247 with defects in cohesion, *smc-3(t2553)* and in *coh-3(gk112); coh-4(tm1857)* double
248 mutants [33–35] did not exhibit germline atrophy phenotypes observed in *gsp-2(yp14)*
249 (Fig. S2, Table S2). Therefore, the late-generation sterility phenotypes of *gsp-2(yp14)*
250 and small RNA mutants are not due to acute loss of meiotic chromosome cohesion.
251

252 **Increased expression of repetitive DNA in sterile *gsp-2(yp14)* and *rsd-6* mutants**

253 One of the main functions of small RNA-mediated genomic silencing is to
254 maintain silencing of repetitive elements and transposons in the germline, thereby
255 protecting genomic integrity [15,19,36]. Previously, we reported that RNA expression of
256 tandem repeat loci was upregulated in late-generation *rsd-2* and *rsd-6* mutants grown at
257 25°C [12]. Because similar levels of germline atrophy and univalents were observed in
258 multiple small RNA pathway mutants and in *gsp-2(yp14)* at sterility, we asked if
259 desilencing of tandem repeats occurred in *gsp-2(yp14)* mutants. We used RNA
260 fluorescence *in situ* hybridization (FISH) to examine the expression of multiple repetitive
261 elements. In wild-type controls grown at 25°C, we detected RNA from tandem repeat
262 sequences using *CeRep59* sense and anti-sense probes in embryos but not in the adult
263 germline or somatic cells, consistent with previous observations (Fig. 3A,B) [12].
264 However, in late-generation *gsp-2(yp14)* and *rsd-6*, robust expression of tandem
265 repeats was observed throughout the soma and germline of adult animals, indicating
266 that tandem repeats become desilenced in these strains (Fig. 3C-F).
267

268 **Small RNA silencing components and *gsp-2* promote germ cell immortality**

bioRxiv preprint doi: https://doi.org/10.1101/273722; this version posted March 1, 2018. The copyright holder for this preprint (which was not certified by peer review) is the author/funder. All rights reserved. No reuse allowed without permission.

269 To study the relationship between *gsp-2(yp14)* and the small RNA nuclear
270 silencing pathway, we created double mutants between *gsp-2(yp14)* and small RNA
271 silencing mutants that display temperature-sensitive defects in germ cell immortality,
272 *hrde-1, nrde-2* and *rsd-6.* Because *gsp-2(yp14)* is a hypomorphic allele, we predicted
273 there would be a similar number of generations to sterility if it were functioning in the
274 small RNA silencing pathway. For *gsp-2(yp14); hrde-1* and *rsd-6; gsp-2(yp14)*, we saw
275 a modest decrease in the number of generations to sterility suggesting a slight additive
276 effect (Fig. 4A,C, Log Rank test: p<.0001). In contrast, *nrde-2; gsp-2(yp14)* double
277 mutants did not differ from the single mutants (Fig. 4B, Log Rank test: p=.06). Together,
278 these results indicate that there is a weak additive effect on transgenerational lifespan
279 when *gsp-2* is combined with *hrde-1* or *rsd-6*, but not when it is combined with *nrde-2*,
280 which promotes the accumulation of stalled RNA polymerase II at loci that are targeted
281 by small RNAs. The modest acceleration observed for some small RNA genomic
282 silencing pathway and *gsp-2(yp14)* double mutants may be consistent with a recent
283 report that indicated that epigenetic silencing marks typically overlap imperfectly for
284 epigenomic silencing mutants, such that both shared and unique targets occur [15].
285

286 **_gsp-2(yp14)_ and _lab-1_ display increased histone H3 phosphorylation**

287 Previously, increased H3S10 phosphorylation was observed when *gsp-2* is
288 deficient [30]. The H3K9me and H3S10p marks can function as a phospho-methyl
289 switch where H3S10 phosphorylation can block some epigenetic regulators, such as
290 HP1, from accessing the adjacent H3K9me mark [37–39]. H3S10 phosphorylation was
291 visible on the condensed chromosomes in the -1 to -3 oocytes in wildtype worms grown

bioRxiv preprint doi: https://doi.org/10.1101/273722; this version posted March 1, 2018. The copyright holder for this preprint (which was not certified by peer review) is the author/funder. All rights reserved. No reuse allowed without permission.

292 at 20°C and 25°C (Fig. 5A). In both early- and late-generation *gsp-2(yp14)* mutant
293 oocytes, H3S10 phosphorylation increased when compared with wildtype controls, with
294 increased levels on chromosomes (Fig. 5B,M). We observed increased levels of H3S10
295 phosphorylation in *lab-1* mutants (Fig. 5C,M), consistent with previous results [25].
296 Increased levels of H3S10p also occurred in *lab-1, rsd-6,* and *hrde-1* but not in *nrde-2*
297 mutants (Fig. 5C-F,M). Late-generation *gsp-2(yp14)* mutant animals grown at 25ºC had
298 a small but significant increase in H3S10 phosphorylation levels compared to *gsp-*
299 *2(yp14)* mutant controls grown at 20ºC (Fig. 5M).

300 PP1 has been previously shown to dephosphorylate a number of histone amino
301 acids, including H3T3 [40]. LAB-1 recruits GSP-2/PP1 to dephosphorylate H3T3, which
302 represses the recruitment of Aurora B/AIR-2 to the long arms of *C. elegans* meiotic
303 chromosomes, which separate in Meiosis II, thereby restricting Aurora B-mediated
304 phosphorylation of H3S10 to meiotic short arms, which separate in Meiosis I [25,26,41].
305 We hypothesized that excess H3T3 phosphorylation could affect the ability of H3K4
306 demethylases to access H3K4 resulting in a Mrt phenotype similar to *rbr-2* or *spr-5*
307 H3K4 demethylase mutants [42]. When we examined H3T3 phosphorylation in wildtype
308 controls, staining was visible in the -1 to -3 oocytes and was localized to the short arms
309 of meiotic chromosomes, the site of chromosome separation at Meiosis I (Fig. 5G-G').
310 The long arms, which do not exhibit staining, are analogous to the centromere in mono-
311 centromeric organisms (Fig. 7). However, in *gsp-2(yp14)* mutants, H3T3p staining was
312 expanded to cover the entire chromosome and was significantly brighter when images
313 where taken under the same conditions (Fig. 5H-H'). In contrast to our H3S10p results,
314 *lab-1* and the small RNA mutants *hrde-1, rsd-6* and *nrde-2* all exhibited increased H3T3

bioRxiv preprint doi: https://doi.org/10.1101/273722; this version posted March 1, 2018. The copyright holder for this preprint (which was not certified by peer review) is the author/funder. All rights reserved. No reuse allowed without permission.

315 phosphorylation signal intensity in the -1 to -3 oocytes, although the signal was still
316 localized properly to the short arms of the meiotic chromosomes (Fig. 5I-L,N).
317 Furthermore, there was a significant increase in H3T3 phosphorylation in the sterile
318 generation of *gsp-2(yp14)* mutants compared to the earlier, fertile generation animals
319 suggesting transgenerational accumulation of H3T3 phosphorylation (Fig. 5N).
320 Together, our results suggest that an increase in phosphorylation of H3T3 but not
321 H3S10 consistently occurs in oocytes of *gsp-2* and small RNA silencing mutants. This
322 defect is sensitive to temperature, as observed for the meiotic chromosome segregation
323 and germ cell immortality defects of *gsp-2(yp14)* (Fig. 1E,F).
324

325 **Small RNA-mediated genome silencing is disrupted in *gsp-2(yp14)***

326 Multiple genes that regulate small RNA-mediated epigenomic silencing promote germ
327 cell immortality, including three genes that are required for a form of transcriptional gene
328 silencing termed nuclear RNA interference, *nrde-1*, *nrde-2* and *nrde-4* [10,12,43]. The
329 response to a dsRNA trigger that targets *lin-26* is dependent on nuclear RNA
330 interference [44]. Control wildtype and *gsp-2* mutant animals displayed a completely
331 penetrant Embryonic Lethality phenotype in response to *lin-26* dsRNA, whereas nuclear
332 RNAi defective mutant *nrde-2* and the RNAi defective mutant *rsd-6* did not (Fig. 6A),
333 indicating that nuclear RNAi within a single generation is normal in the *gsp-2* mutant.
334 Small RNAs can trigger RNAi inheritance [10,13], where silencing of a gene in
335 response to siRNAs can be transmitted for multiple generations. Transgenerational
336 RNAi inheritance can occur when endogenous genes are targeted by dsRNA triggers
337 [45], but this can also happen when GFP reporter transgenes are targeted by small

bioRxiv preprint doi: https://doi.org/10.1101/273722; this version posted March 1, 2018. The copyright holder for this preprint (which was not certified by peer review) is the author/funder. All rights reserved. No reuse allowed without permission.

338 RNAs derived from *GFP*. We tested the transgene *cpIs12* and found that it was silenced
339 in response to GFP siRNAs and that silencing of this transgene was inherited for up to 4
340 generations after removal from the dsRNA trigger (Fig. 6B). In contrast, GFP expression
341 in *gsp-2(yp14)*; *cpIs12* was initially silenced but silencing was not inherited over multiple
342 generations (Fig. 6B), suggesting that *gsp-2* plays a role in RNAi inheritance.
343 Propagation of GFP or mCherry transgenes in the heterozygous state for multiple
344 generations can elicit strong transgene silencing [21]. We found that the transgene
345 *cpIs12* was progressively silenced in the population over the course of several
346 generations until fully silenced by generation 5 (Fig. 6C). In contrast, when *cpIs12* was
347 placed in a *gsp-2(yp14)* genetic background and propagated in a heterozygous state,
348 we found that *cpIs12* was initially weakly silenced and that genomic silencing never
349 became fully penetrant (Fig. 6C). Together, the above data indicate that *gsp-2* promotes
350 transgenerational small RNA-induced genome silencing.
351
352 **Small RNA dysfunction in *gsp-2* mutants**
353 Given that small RNA-mediated genome silencing is dysfunctional in *gsp-2(yp14)*
354 mutants, we asked if small RNA populations were perturbed by preparing RNA from
355 early- and late-generation wildtype, *gsp-2(yp14)*, *rsd-6* and *spr-5* mutants grown at
356 either 20°C or 25°C. *spr-5* encodes an H3K4 demethylase that promotes Germ Cell
357 Immortality at 25°C, similar to *rsd-6* and *gsp-2* mutants [42]. Small RNA libraries were
358 prepared and subjected to high throughput sequencing, and we then examined levels of
359 22G RNAs that are 22 nucleotides in length beginning with a 5' guanine, as 22G RNAs
360 are the major effectors of genomic silencing in *C. elegans* [5,46]. Analysis of the small

bioRxiv preprint doi: https://doi.org/10.1101/273722; this version posted March 1, 2018. The copyright holder for this preprint (which was not certified by peer review) is the author/funder. All rights reserved. No reuse allowed without permission.

361 RNA data revealed that *spr-5* and *rsd-6* share some genes with reduced levels of 22G
362 RNAs with increasing generations, but there are other genes that show dissimilar
363 behavior for each individual mutant. This suggests that *spr-5* may act both in
364 conjunction with *rsd-6* and in a separate pathway to promote germline immortality. In
365 contrast, 22G RNAs from *gsp-2(yp14)* showed strong similarities to those of *spr-5*
366 mutants but showed little similarity to 22G RNA changes observed for *rsd-6* mutants
367 (Fig. 6D and Fig. S3), suggesting that *gsp-2* may act in a separate pathway from *rsd-6*,
368 in agreement with the results from epistasis experiments above. As a control, there is
369 little coherent change in late-generation versus early generation N2 wildtype that
370 overlaps with *gsp-2(yp14)* (Fig. S3). As germ cell immortality is promoted in part by
371 primary siRNAs termed piRNAs that interact with the Piwi Argonaute protein PRG-1 [8],
372 we also examined piRNA populations, which are enriched for 21 nucleotide RNAs that
373 begin with a 5' uracil (21U RNAs) [6,7,9] and found that these were normal (Fig. 6E).
374

375 **Discussion**

376 We demonstrate for the first time that *gsp-2* and *lab-1* are required for germ cell
377 immortality at 25°C as strains deficient for these proteins can be passaged for a number
378 of generations before becoming sterile (Fig. 1C,D). Although PP1 is a general protein
379 phosphatase with roles in a number of cellular processes including mitosis and meiosis
380 [24], we identified a separation-of-function allele of *gsp-2* that displayed an X
381 chromosome non-disjunction phenotype that was specific for meiosis (Fig. 1B,G). The
382 incidence of both X chromosome loss and inviable embryos, which are likely aneuploid
383 for autosomes, was exacerbated at high temperature (Fig. 1A,B), suggesting that this

bioRxiv preprint doi: https://doi.org/10.1101/273722; this version posted March 1, 2018. The copyright holder for this preprint (which was not certified by peer review) is the author/funder. All rights reserved. No reuse allowed without permission.

384 meiotic chromosome segregation defect could contribute to the temperature-sensitive
385 nature of the Mrt phenotype of *gsp-2(yp14)*. Consistently, PP1/GSP-2 is recruited to
386 meiotic chromosomes by the *C. elegans*-specific protein LAB-1, and we found that
387 deficiency for *lab-1* elicited transgenerational sterility accompanied by adult germ cell
388 degeneration phenotypes that were observed in sterile small RNA silencing mutants
389 (Fig. 1F and Fig 2). Together, these results indicate that LAB-1 and GSP-2/PP1 define a
390 step during meiosis that is critical for potentiating transgenerational small RNA-
391 mediated genome silencing and germ cell immortality (Fig. 7A).

392 LAB-1 localizes to the interface between homologous chromosomes during
393 pachytene, and LAB-1 recruits GSP-2 to nuclei during early stages of meiosis (Fig. 7A)
394 (de Carvalho et al., 2008; Tzur et al., 2012). Moreover, deficiency for LAB-1 perturbs the
395 pairing of homologous chromosomes during meiosis, which has been attributed to a
396 defect in the cohesion of sister chromatids (Tzur et al., 2012). We suggest that a
397 previously undescribed function of LAB-1/GSP-2, potentially related to the pairing of
398 homologous chromosomes, may act at the interface between homologs to promote
399 small RNA-mediated epigenomic silencing (Fig. 7A). We found that persistent
400 transgenerational discontinuities in the pairing of homologous chromosomes during
401 meiosis, caused by hemizygous transgenes, can promote transgene silencing in a
402 manner that depends on GSP-2 (Fig. 6C, Fig. 7C). This hemizygous transgene
403 silencing process occurs in a manner that depends *prg-1*/piRNAs as well as
404 downstream factors that promote second siRNA biogenesis [21]. However, we found
405 that piRNA levels were normal in *gsp-2(yp14)* mutants, and also that late-generation
406 *gsp-2(yp14)* strains displayed changes in 22G RNA levels that were similar to those of

bioRxiv preprint doi: https://doi.org/10.1101/273722; this version posted March 1, 2018. The copyright holder for this preprint (which was not certified by peer review) is the author/funder. All rights reserved. No reuse allowed without permission.

407 *spr-5* histone H3K4 demethylase mutants but not to those of *rsd-6* small RNA
408 biogenesis mutants (Fig. 6D and Fig. S3). Moreover, epistasis analysis indicated that
409 there is a weak additive effect when *gsp-2* is combined with the nuclear Argonaute
410 *hrde-1* or the small RNA biogenesis factor *rsd-6,* but no additive effect when *gsp-2* is
411 combined with *nrde-2* (Fig. 4), which like *spr-5* functions downstream of siRNAs to
412 promote transcriptional silencing [47]. The parallel with *spr-5* mutant small RNA levels
413 suggests that GSP-2 help to integrate histone silencing modifications with the response
414 to small RNAs (Fig. 7B). An intriguing possibility is that hemizygous transgenes could
415 create a structural discontinuity between homologous chromosomes that alter the
416 normal meiotic function of LAB-1/GSP-2, creating an environment where the
417 chromosome silencing machinery can respond to small RNAs (Fig. 7C). Alternatively,
418 the presence of a homologous allele could provide protection from silencing [48–50].
419 These possibilities are consistent with a role for small RNA-mediated genome silencing
420 in responding to structures of *de novo* transposon insertions that present a threat to
421 genomic integrity and that might create small hemizygous chromosome pairing
422 aberrations during meiosis, which would be structurally analogous to hemizygous
423 transgenes (Fig. 7C).

424 Consistent with our results, an allele of the *Drosophila* Protein Phosphatase 1
425 gene, *Su var (3) 6*, was identified as a suppressor of position-effect variegation, which
426 relieves epigenetic silencing of a transcriptionally active gene that is placed adjacent to
427 a segment of heterochromatin [29]. As position-effect variegation is promoted by small
428 RNA-mediated genome silencing in plants and animals [51,52], we conclude that PP1 is
429 likely to play a conserved role in this epigenomic silencing process. It has been

bioRxiv preprint doi: https://doi.org/10.1101/273722; this version posted March 1, 2018. The copyright holder for this preprint (which was not certified by peer review) is the author/funder. All rights reserved. No reuse allowed without permission.

430 suggested that the heterochromatin defect of *Su var (3) 6* mutants could reflect a direct
431 role of PP1 in dephosphorylation of H3S10p, a mark that results in dissociation of
432 Heterochromatin Protein 1 from heterochromatin [40,41]. Moreover, human PP1 has
433 been shown to dephosphorylate H3T3p, this function is also carried out by *C. elegans*
434 GSP-2 during meiosis [40,41]. One or both of these silencing marks could be relevant to
435 meiotic small RNA-mediated genome silencing. Interestingly, the cohesin complex has
436 been found to be recruited to silent chromatin, but in most cases has not been found to
437 be necessary for genomic silencing [53]. As GSP-2 plays a role in protecting cohesin
438 from being prematurely removed, it is likely localized to silent chromatin where it may
439 play a role in maintaining silencing.

440 We observed increased H3T3 and H3S10 phosphorylation in mature oocytes of
441 *gsp-2(yp14)* mutants as well as in small RNA genome silencing mutants. While the H3
442 phosphorylation defects that we observed were mildly sensitive to temperature, *gsp-*
443 *2(yp14)* displayed more pronounced H3 phosphorylation defects that spread along the
444 length of meiotic chromosomes, whereas small RNA mutants displayed proper H3
445 phosphorylation localization whose intensity was consistently stronger than for wildtype
446 controls for H3T3 but not for H3S10 (Fig. 5). Given that LAB-1/GSP-1 localize to sister
447 chromosomes in mature oocytes that are arrested in Meiosis I, where homologous
448 chromosomes are held together only by crossovers, we propose that the role of LAB-
449 1/GSP-2 in genome silencing may be at earlier stages of meiosis where the homologs
450 are paired in a manner that might be capable of responding to discontinuities between
451 homologs. We suggest that the changes in H3T3 phosphorylation of genome silencing
452 mutants could reflect an indirect effect of dysregulation of heterochromatin, for example

bioRxiv preprint doi: https://doi.org/10.1101/273722; this version posted March 1, 2018. The copyright holder for this preprint (which was not certified by peer review) is the author/funder. All rights reserved. No reuse allowed without permission.

453 a response to altered levels of genome-wide levels of H3K9 methylation could affect the
454 activity of protein that functions in the context of heterochromatin, such as the H3T3
455 kinase Haspin [43]. As H3T3 phosphorylation is constitutively disrupted in maturing
456 oocytes of the genomic silencing mutants we studied, especially in *gsp-2* and *lab-1*
457 mutants, it is also possible that this phosphorylation mark plays a role in genomic
458 silencing itself.

459 While piRNAs and associated small RNA-mediated genome silencing have been
460 well defined as functioning primarily in the germ line, our study suggests a novel
461 connection between a meiotic process where Piwi-associated small RNAs scan
462 homologous chromosomes for relatively small changes to their primary structure and
463 germ cell immortality. This concept is well supported by work in other organisms,
464 particularly in various fungi and *Drosophila*, where it has been shown that regions of
465 heterozygosity are prone to silencing during meiosis in a small RNA dependent manner
466 (reviewed by [20]). It is also possible that the GSP-2 protein phosphatase promotes
467 small RNA-mediated genome silencing by directly modifying histones or a component of
468 the genome silencing machinery that responds to small RNAs. In principle, our study
469 defines a meiotic process that may intimately link transgenerational small RNA-
470 mediated genome silencing with the structure of paired homologous chromosomes
471 during meiosis. Given that endogenous small RNAs promote germ line stem cell
472 maintenance, oogenesis and meiosis itself [54,55], we suggest that small RNA
473 pathways and germ cell development have evolved to become mutually reinforcing
474 processes.
475

bioRxiv preprint doi: https://doi.org/10.1101/273722; this version posted March 1, 2018. The copyright holder for this preprint (which was not certified by peer review) is the author/funder. All rights reserved. No reuse allowed without permission.

476 **Materials and Methods**

477 **Strains:**
478 All strains were cultured at 20°C or 25°C on Nematode Growth Medium (NGM) plates
479 seeded with *E. coli* OP50. Strains used include Bristol N2 wild type, *gsp-2(tm301) III,*
480 *gsp-2(yp14) III, lab-1(tm1791) I, cpIs12[Pmex-5::GFP::tbb-2 3'UTR + unc-119(+)] II, hrde-*
481 *1(tm1200) III, rsd-6(yp11) I, nrde-2(gg95) II, rbr-2(tm1231) IV, smc-3(t2553) III, coh-*
482 *4(tm1857) V, coh-3(gk112) V, air-2(or207) I, unc-32(e189) III, unc-13(e450) I, unc-*
483 *24(e1172) IV.*
484

485 **Germline Mortality Assay:**
486 Worms were assessed for the Mortal Germline phenotype using the assay previously
487 described [2]. L1 or L2 larvae were transferred for all assays. After passaging plates
488 that yielded no additional L1 animals were marked as sterile. Log-rank analysis was
489 used to determine differences of transgenerational lifespan between strains.
490

491 **DAPI staining:**
492 DAPI staining was performed as previously described. L4 larvae were selected from
493 sibling plates and sterile adults were singled as late L4s, observed 24 hours later for
494 confirmed sterility, and then stained 48 hours after collection.

495 **RNA FISH:**
496 DNA oligonucleotide probes coupled with a 5′ Cy5 fluorophore were used to detect
497 repetitive element expression. The four probes used in this study were as follows:
498 tttctgaaggcagtaattct, *CeRep59* on chromosome *I* (located at 4281435–4294595 nt);
499 agaattactgccttcagaaa, antisense *CeRep59* on chromosome *I*; caactgaatccagctcctca,
500 chromosome *V* tandem repeat (located at 8699155–8702766 nt); and
501 gcttaagttcagcgggtaat, 26S rRNA. The strains used for RNA FISH experiments were *rsd-*
502 *6(yp11)*, *gsp-2(yp14)*, and N2 Bristol wild type. Staining was performed as described by
503 Sakaguchi et al., 2014.

504 **Immunofluorescence:**
505 Adult hermaphrodites raised at 20°C or 25°C were dissected in M9 buffer and flash
506 frozen on dry ice before fixation for 1 min in methanol at -20°C. After washing in PBS
507 supplemented with 0.1% Tween-20 (PBST), primary antibody diluted in in PBST was
508 used to immunostain overnight at 4 °C in a humid chamber. Primaries used were 1:500
509 pH3S10 (Millipore, 06570), 1:4000 pH3T3 (Cell Signaling, D5G1I, Rabbit) and 1:50
510 OIC1D4 (Developmental Studies Hybridoma Bank). Secondary antibody staining was
511 performed by using an Cy3 donkey anti-mouse or Cy-5 donkey anti-rabbit overnight at
512 4°C. All images were obtained using a LSM 710 laser scanning confocal and were
513 taken using same settings as control samples. Images processed using ImageJ.
514 Intensity quantification was done by measuring total fluorescence in individual
515 condensed chromosomes and subtracting the background levels obtained from mitotic
516 nuclei as nucleoplasm levels varied greatly.
517

518 **RNAi Assays:** N2 wildtype, *gsp-2*, *rsd-6* and *nrde-2* animals were grown on *lin-26* RNAi
519 clones and the progeny of 10 worms each were scored for Embryonic Lethality.

bioRxiv preprint doi: https://doi.org/10.1101/273722; this version posted March 1, 2018. The copyright holder for this preprint (which was not certified by peer review) is the author/funder. All rights reserved. No reuse allowed without permission.

520 **Transgene silencing assay:** *cpIs12* and *gsp-2; cpIs12* worms were scored for GFP
521 expression on NGM plates and then transferred to RNAi plates targeting GFP. The next
522 generation (that was laid on GFPi plates) were scored for GFP expression and their
523 sisters were removed and transferred back to NGM plates. Worms were propagated for
524 multiple generations on NGM and scored each time for GFP expression. Both GFP
525 reporter *gsp-2* doubles were created by marking with *dpy-17*.

526 **Heterozygous transgene silencing:** *cpIs12* was maintained as a heterozygote over
527 *dpy-10 unc-4* while in *gsp-2; cpIs12* doubles, *gsp-2* remained mutant for the entire
528 assay and *cpIs12* was balanced over *dpy-10 unc-4*.
529
530 **Genome sequence analysis:**
531 Paired sequence reads (2X100 nucleotide long) were mapped to the C. elegans reference
532 genome version WS230 (www.wormbase.org) using the short-read aligner BWA [56]. The
533 resulting alignment files were sorted and indexed with the help of the SAMtools toolbox
534 [57]. The average sequencing depths for the mutant and wild-type N2 strains were 116x
535 and 71x, respectively. Single-nucleotide variants (SNVs) were identified and filtered with
536 SAMtools and annotated with a custom Perl script using gene information downloaded from
537 WormBase WS230. Candidate SNVs in the mutant strain already present in the N2 strain
538 were eliminated from further consideration.

539 The raw sequence data from this study have been submitted to the NCBI BioProject
540 (http://www.ncbi.nlm.nih.gov/bioproject) under accession number PRJNA395732 and can
541 be accessed from the Sequence Read Archive (SRA; https://www.ncbi.nlm.nih.gov/sra) with
542 accession number SRP113543.

543 **Small RNA Sequence Analysis**
544 5' independent small RNA sequencing was performed as described previously [13],
545 using one repeat for each time-point of N2 WT, *rsd-6* and *spr-5* at 25°C. Custom Perl
546 scripts were used to select different small RNA species from the library. To map small
547 RNA sequences to genes, reads were aligned to the *C. elegans* ce6 genome using
548 Bowtie, Version 0.12.7, requiring perfect matches [58]. Data was normalized to the total
549 number of aligned reads and 1 was added to the number of reads mapping to each
550 gene to avoid division by zero errors. To map 22G sequences to transposons and
551 tandem repeats, direct alignment to the transposon consensus sequences, downloaded
552 from Repbase (Ver 17.05) or repeats obtained from the ce6 genome (WS190)
553 annotations downloaded from UCSC as above, was performed using Bowtie allowing up
554 to two mismatches and reporting only the best match. Uncollapsed fasta files were used
555 for these alignments to compensate for the problem of multiple identical matches. Data
556 was normalized to the total library size and 1 was added to the number of reads
557 mapping to each feature to avoid division by zero errors. In order to analyze data from
558 *rsd-2* mutants grown at 20°C [59], Fasta files were downloaded from the Gene
559 Expression Omnibus and uncollapsed using a custom Perl script before aligning to
560 transposons or tandem repeats as above. Analysis of data was carried out using the R
561 statistical language [60].
562

bioRxiv preprint doi: https://doi.org/10.1101/273722; this version posted March 1, 2018. The copyright holder for this preprint (which was not certified by peer review) is the author/funder. All rights reserved. No reuse allowed without permission.

563 **Acknowledgements**
564 We thank Jonathan Hodgkin for mapping assistance and members of the S.A.
565 laboratory for critical review of the manuscript. Some strains were provided by the
566 Caenorhabditis Genetics Center, which is funded by National Institutes of Health Office
567 of Research Infrastructure Programs (P40 OD010440). Work in the DM laboratory is
568 funded by the Canadian Institute for Health Research. This work was supported by
569 National Institute of Health grant numbers F32 GM120809 (K.B) and RO1 GM083048
570 (S.A). SA is a recipient of a Senior Scholar in Aging Award from the Ellison Medical
571 Foundation. Work in PS laboratory is funded by the Medical Research Council. PS
572 holds an Imperial College Research Fellowship.
573

574 **References**

575 1. Sharpless NE, DePinho RA. How stem cells age and why this makes us grow old.
576 Nat Rev Mol Cell Biol [Internet]. 2007 Sep [cited 2017 Jun 26];8(9):703–13.
577 Available from: http://www.ncbi.nlm.nih.gov/pubmed/17717515
578 2. Ahmed S, Hodgkin J. MRT-2 checkpoint protein is required for germline
579 immortality and telomere replication in C. elegans. Nature [Internet]. 2000 Jan 13
580 [cited 2015 Nov 30];403(6766):159–64. Available from:
581 http://www.ncbi.nlm.nih.gov/pubmed/10646593
582 3. Armanios M, Blackburn EH. The telomere syndromes. Nat Rev Genet [Internet].
583 2012 Sep 11 [cited 2017 Jun 26];13(10):693–704. Available from:
584 http://www.ncbi.nlm.nih.gov/pubmed/22965356
585 4. Meier B, Clejan I, Liu Y, Lowden M, Gartner A, Hodgkin J, et al. trt-1 is the
586 Caenorhabditis elegans catalytic subunit of telomerase. PLoS Genet [Internet].
587 2006 Feb 10 [cited 2015 Nov 16];2(2):e18. Available from:
588 http://dx.plos.org/10.1371/journal.pgen.0020018
589 5. Bagijn MP, Goldstein LD, Sapetschnig A, Weick EM, Bouasker S, Lehrbach NJ, et
590 al. Function, targets, and evolution of Caenorhabditis elegans piRNAs. Science
591 (80-) [Internet]. 2012 Aug 3 [cited 2017 Jun 26];337(6094):574–8. Available from:
592 http://www.ncbi.nlm.nih.gov/pubmed/22700655
593 6. Batista PJ, Ruby JG, Claycomb JM, Chiang R, Fahlgren N, Kasschau KD, et al.
594 PRG-1 and 21U-RNAs interact to form the piRNA complex required for fertility in
595 C. elegans. Mol Cell [Internet]. 2008 Jul 11 [cited 2017 Jul 5];31(1):67–78.
596 Available from: http://www.ncbi.nlm.nih.gov/pubmed/18571452
597 7. Das PP, Bagijn MP, Goldstein LD, Woolford JR, Lehrbach NJ, Sapetschnig A, et
598 al. Piwi and piRNAs Act Upstream of an Endogenous siRNA Pathway to
599 Suppress Tc3 Transposon Mobility in the Caenorhabditis elegans Germline. Mol
600 Cell [Internet]. 2008 Jul 11 [cited 2017 Jun 26];31(1):79–90. Available from:
601 http://www.ncbi.nlm.nih.gov/pubmed/18571451
602 8. Simon M, Sarkies P, Ikegami K, Doebley A-L, Goldstein LD, Mitchell J, et al.
603 Reduced insulin/IGF-1 signaling restores germ cell immortality to Caenorhabditis
604 elegans Piwi mutants. Cell Rep [Internet]. 2014 May 8 [cited 2015 Nov
605 11];7(3):762–73. Available from:
606 http://www.pubmedcentral.nih.gov/articlerender.fcgi?artid=4049074&tool=pmcentr

bioRxiv preprint doi: https://doi.org/10.1101/273722; this version posted March 1, 2018. The copyright holder for this preprint (which was not certified by peer review) is the author/funder. All rights reserved. No reuse allowed without permission.

607 ez&rendertype=abstract
608 9. Wang G, Reinke V. A C. elegans Piwi, PRG-1, Regulates 21U-RNAs during
609 Spermatogenesis. Curr Biol [Internet]. 2008 Jun 24 [cited 2018 Feb
610 6];18(12):861–7. Available from: http://www.ncbi.nlm.nih.gov/pubmed/18501605
611 10. Buckley BA, Burkhart KB, Gu SG, Spracklin G, Kershner A, Fritz H, et al. A
612 nuclear Argonaute promotes multigenerational epigenetic inheritance and
613 germline immortality. Nature [Internet]. 2012 Jul 18 [cited 2017 Jun
614 26];489(7416):447–51. Available from:
615 http://www.nature.com/doifinder/10.1038/nature11352
616 11. Juliano C, Wang J, Lin H. Uniting Germline and Stem Cells: The Function of Piwi
617 Proteins and the piRNA Pathway in Diverse Organisms. Annu Rev Genet
618 [Internet]. 2011 Dec 15 [cited 2017 Jun 26];45(1):447–69. Available from:
619 http://www.ncbi.nlm.nih.gov/pubmed/21942366
620 12. Sakaguchi A, Sarkies P, Simon M, Doebley A-L, Goldstein LD, Hedges A, et al.
621 Caenorhabditis elegans RSD-2 and RSD-6 promote germ cell immortality by
622 maintaining small interfering RNA populations. Proc Natl Acad Sci U S A
623 [Internet]. 2014 Oct 14 [cited 2017 Jun 26];111(41):E4323-31. Available from:
624 http://www.ncbi.nlm.nih.gov/pubmed/25258416
625 13. Ashe A, Sapetschnig A, Weick E-M, Mitchell J, Bagijn MP, Cording AC, et al.
626 piRNAs can trigger a multigenerational epigenetic memory in the germline of C.
627 elegans. Cell [Internet]. 2012 Jul 6 [cited 2017 Jun 26];150(1):88–99. Available
628 from: http://www.ncbi.nlm.nih.gov/pubmed/22738725
629 14. Burkhart KB, Guang S, Buckley BA, Wong L, Bochner AF, Kennedy S. A pre-
630 mRNA-associating factor links endogenous siRNAs to chromatin regulation. PLoS
631 Genet [Internet]. 2011 Aug [cited 2017 Jun 26];7(8):e1002249. Available from:
632 http://www.ncbi.nlm.nih.gov/pubmed/21901112
633 15. McMurchy AN, Stempor P, Gaarenstroom T, Wysolmerski B, Dong Y,
634 Aussianikava D, et al. A team of heterochromatin factors collaborates with small
635 RNA pathways to combat repetitive elements and germline stress. Elife [Internet].
636 2017 Mar 15 [cited 2017 Jun 26];6. Available from:
637 http://elifesciences.org/lookup/doi/10.7554/eLife.21666
638 16. Spracklin G, Fields B, Wan G, Vijayendran D, Wallig A, Shukla A, et al.
639 Identification and Characterization of Caenorhabditis elegans RNAi Inheritance
640 Machinery. Genetics [Internet]. 2017 [cited 2017 Jun 29]; Available from:
641 http://www.genetics.org/content/early/2017/05/22/genetics.116.198812
642 17. Luteijn MJ, van Bergeijk P, Kaaij LJT, Almeida MV, Roovers EF, Berezikov E, et
643 al. Extremely stable Piwi-induced gene silencing in *Caenorhabditis elegans*.
644 EMBO J [Internet]. 2012 Aug 15 [cited 2017 Jun 26];31(16):3422–30. Available
645 from: http://emboj.embopress.org/cgi/doi/10.1038/emboj.2012.213
646 18. Shirayama M, Seth M, Lee H-C, Gu W, Ishidate T, Conte D, et al. piRNAs Initiate
647 an Epigenetic Memory of Nonself RNA in the C. elegans Germline. Cell [Internet].
648 2012 Jul 6 [cited 2017 Jun 26];150(1):65–77. Available from:
649 http://www.ncbi.nlm.nih.gov/pubmed/22738726
650 19. Zeller P, Padeken J, van Schendel R, Kalck V, Tijsterman M, Gasser SM. Histone
651 H3K9 methylation is dispensable for Caenorhabditis elegans development but
652 suppresses RNA:DNA hybrid-associated repeat instability. Nat Genet [Internet].

bioRxiv preprint doi: https://doi.org/10.1101/273722; this version posted March 1, 2018. The copyright holder for this preprint (which was not certified by peer review) is the author/funder. All rights reserved. No reuse allowed without permission.

653 2016 Sep 26 [cited 2017 Jun 29];48(11):1385–95. Available from:
654 http://www.ncbi.nlm.nih.gov/pubmed/27668659
655 20. Kelly WG, Aramayo R. Meiotic silencing and the epigenetics of sex. Chromosom
656 Res [Internet]. 2007 [cited 2018 Jan 29];(15):633–651. Available from:
657 https://link.springer.com/content/pdf/10.1007/s10577-007-1143-0.pdf
658 21. Leopold LE, Heestand BN, Seong S, Shtessel L, Ahmed S. Lack of pairing during
659 meiosis triggers multigenerational transgene silencing in Caenorhabditis elegans.
660 Proc Natl Acad Sci U S A [Internet]. 2015 May 19 [cited 2015 Nov
661 16];112(20):E2667-76. Available from:
662 http://www.ncbi.nlm.nih.gov/pubmed/25941370
663 22. Chu DS, Liu H, Nix P, Wu TF, Ralston EJ, Yates III JR, et al. Sperm chromatin
664 proteomics identifies evolutionarily conserved fertility factors. Nature [Internet].
665 2006 Sep 7 [cited 2017 Jun 26];443(7107):101–5. Available from:
666 http://www.ncbi.nlm.nih.gov/pubmed/16943775
667 23. Wu J -c., Go AC, Samson M, Cintra T, Mirsoian S, Wu TF, et al. Sperm
668 Development and Motility are Regulated by PP1 Phosphatases in Caenorhabditis
669 elegans. Genetics [Internet]. 2012 Jan 1 [cited 2017 Jun 26];190(1):143–57.
670 Available from: http://www.ncbi.nlm.nih.gov/pubmed/22042574
671 24. Ceulemans H, Bollen M. Functional Diversity of Protein Phosphatase-1, a Cellular
672 Economizer and Reset Button. Physiol Rev [Internet]. 2004 [cited 2017 Jun
673 26];84(1). Available from: http://physrev.physiology.org/content/84/1/1
674 25. de Carvalho CE, Zaaijer S, Smolikov S, Gu Y, Schumacher JM, Colaiacovo MP.
675 LAB-1 antagonizes the Aurora B kinase in C. elegans. Genes Dev [Internet]. 2008
676 Oct 15 [cited 2017 Jun 12];22(20):2869–85. Available from:
677 http://www.ncbi.nlm.nih.gov/pubmed/18923084
678 26. Tzur YB, Egydio de Carvalho C, Nadarajan S, Van Bostelen I, Gu Y, Chu DS, et
679 al. LAB-1 Targets PP1 and Restricts Aurora B Kinase upon Entrance into Meiosis
680 to Promote Sister Chromatid Cohesion. Hawley RS, editor. PLoS Biol [Internet].
681 2012 Aug 21 [cited 2017 Jun 26];10(8):e1001378. Available from:
682 http://dx.plos.org/10.1371/journal.pbio.1001378
683 27. Hodgkin J, Horvitz HR, Brenner S. Nondisjunction Mutants of the Nematode
684 CAENORHABDITIS ELEGANS. Genetics [Internet]. 1979 Jan [cited 2017 Jun
685 28];91(1):67–94. Available from: http://www.ncbi.nlm.nih.gov/pubmed/17248881
686 28. Sassa T, Ueda-Ohba H, Kitamura K, Harada S, Hosono R. Role of
687 Caenorhabditis elegans protein phosphatase type 1, CeGLC-7B,in metaphase to
688 anaphase transition during embryonic development. Exp Cell Res [Internet]. 2003
689 Jul 15 [cited 2017 Jun 28];287(2):350–60. Available from:
690 http://linkinghub.elsevier.com/retrieve/pii/S0014482703001575
691 29. Dombradi V, Axton JM, Barker HM, Cohen PTW. Protein phosphatase 1 activity in
692 Drosophila mutants with abnormalities in mitosis and chromosome condensation.
693 FEBS Lett [Internet]. 1990 Nov 26 [cited 2017 Jun 26];275(1–2):39–43. Available
694 from: http://doi.wiley.com/10.1016/0014-5793%2890%2981434-P
695 30. Hsu J-Y, Sun Z-W, Li X, Reuben M, Tatchell K, Bishop DK, et al. Mitotic
696 Phosphorylation of Histone H3 Is Governed by Ipl1/aurora Kinase and Glc7/PP1
697 Phosphatase in Budding Yeast and Nematodes logical changes on the DNA
698 template in an energy. Cell [Internet]. 2000 [cited 2017 Jun 12];102:279–91.

bioRxiv preprint doi: https://doi.org/10.1101/273722; this version posted March 1, 2018. The copyright holder for this preprint (which was not certified by peer review) is the author/funder. All rights reserved. No reuse allowed without permission.

699 Available from:
700 https://pdfs.semanticscholar.org/ddf3/60514ab900f10f1815057170a4428fea0279.
701 pdf
702 31. Watanabe Y. Shugoshin: guardian spirit at the centromere. Curr Opin Cell Biol
703 [Internet]. 2005 Dec [cited 2017 Jul 5];17(6):590–5. Available from:
704 http://www.ncbi.nlm.nih.gov/pubmed/16229998
705 32. Hamant O, Golubovskaya I, Meeley R, Fiume E, Timofejeva L, Schleiffer A, et al.
706 A REC8-Dependent Plant Shugoshin Is Required for Maintenance of Centromeric
707 Cohesion during Meiosis and Has No Mitotic Functions. Curr Biol [Internet]. 2005
708 May 24 [cited 2017 Jul 5];15(10):948–54. Available from:
709 http://www.ncbi.nlm.nih.gov/pubmed/15916952
710 33. Severson AF, Ling L, van Zuylen V, Meyer BJ. The axial element protein HTP-3
711 promotes cohesin loading and meiotic axis assembly in C. elegans to implement
712 the meiotic program of chromosome segregation. Genes Dev [Internet]. 2009 Aug
713 1 [cited 2017 Jun 26];23(15):1763–78. Available from:
714 http://genesdev.cshlp.org/cgi/doi/10.1101/gad.1808809
715 34. Hagstrom KA, Holmes VF, Cozzarelli NR, Meyer BJ. C. elegans condensin
716 promotes mitotic chromosome architecture, centromere organization, and sister
717 chromatid segregation during mitosis and meiosis. Genes Dev [Internet]. 2002
718 Mar 15 [cited 2017 Jun 26];16(6):729–42. Available from:
719 http://www.ncbi.nlm.nih.gov/pubmed/11914278
720 35. Baudrimont A, Penkner A, Woglar A, Mamnun YM, Hulek M, Struck C, et al. A
721 New Thermosensitive smc-3 Allele Reveals Involvement of Cohesin in
722 Homologous Recombination in C. elegans. Polymenis M, editor. PLoS One
723 [Internet]. 2011 Sep 21 [cited 2017 Jun 26];6(9):e24799. Available from:
724 http://dx.plos.org/10.1371/journal.pone.0024799
725 36. Holoch D, Moazed D. RNA-mediated epigenetic regulation of gene expression.
726 Nat Rev Genet [Internet]. 2015 Jan 2 [cited 2017 Jun 26];16(2):71–84. Available
727 from: http://www.nature.com/doifinder/10.1038/nrg3863
728 37. Sabbattini P, Canzonetta C, Sjoberg M, Nikic S, Georgiou A, Kemball-Cook G, et
729 al. A novel role for the Aurora B kinase in epigenetic marking of silent chromatin in
730 differentiated postmitotic cells. EMBO J [Internet]. 2007 Nov 14 [cited 2017 Jun
731 26];26(22):4657–69. Available from:
732 http://www.ncbi.nlm.nih.gov/pubmed/17948062
733 38. Sabbattini P, Sjoberg M, Nikic S, Frangini A, Holmqvist P-H, Kunowska N, et al.
734 An H3K9/S10 methyl-phospho switch modulates Polycomb and Pol II binding at
735 repressed genes during differentiation. Mol Biol Cell [Internet]. 2014 Mar [cited
736 2017 Jun 26];25(6):904–15. Available from:
737 http://www.ncbi.nlm.nih.gov/pubmed/24430871
738 39. Jeong YS, Cho S, Park JS, Ko Y, Kang Y-K. Phosphorylation of serine-10 of
739 histone H3 shields modified lysine-9 selectively during mitosis. Genes to Cells
740 [Internet]. 2010 Mar [cited 2017 Jun 26];15(3):181–92. Available from:
741 http://www.ncbi.nlm.nih.gov/pubmed/20070858
742 40. Qian J, Lesage B, Beullens M, Van Eynde A, Bollen M. PP1/Repo-Man
743 Dephosphorylates Mitotic Histone H3 at T3 and Regulates Chromosomal Aurora
744 B Targeting. Curr Biol [Internet]. 2011 May 10 [cited 2018 Jan 28];21(9):766–73.

bioRxiv preprint doi: https://doi.org/10.1101/273722; this version posted March 1, 2018. The copyright holder for this preprint (which was not certified by peer review) is the author/funder. All rights reserved. No reuse allowed without permission.

745 Available from: http://www.ncbi.nlm.nih.gov/pubmed/21514157
746 41. Sato-Carlton A, Nakamura-Tabuchi C, Chartrand SK, Uchino T, Carlton PM.
747 Phosphorylation of the synaptonemal complex protein SYP-1 promotes meiotic
748 chromosome segregation. J Cell Biol [Internet]. 2017 Dec 8 [cited 2018 Jan
749 28];jcb.201707161. Available from:
750 http://www.ncbi.nlm.nih.gov/pubmed/29222184
751 42. Alvares SM, Mayberry GA, Joyner EY, Lakowski B, Ahmed S. H3K4 demethylase
752 activities repress proliferative and postmitotic aging. Aging Cell [Internet]. 2014
753 Apr [cited 2017 Jun 26];13(2):245–53. Available from:
754 http://www.ncbi.nlm.nih.gov/pubmed/24134677
755 43. Burton NO, Burkhart KB, Kennedy S. Nuclear RNAi maintains heritable gene
756 silencing in Caenorhabditis elegans. Proc Natl Acad Sci U S A [Internet]. 2011
757 Dec 6 [cited 2017 Jun 26];108(49):19683–8. Available from:
758 http://www.ncbi.nlm.nih.gov/pubmed/22106253
759 44. Guang S, Bochner AF, Pavelec DM, Burkhart KB, Harding S, Lachowiec J, et al.
760 An Argonaute Transports siRNAs from the Cytoplasm to the Nucleus. Science
761 (80-) [Internet]. 2008 Jul 25 [cited 2018 Feb 21];321(5888):537–41. Available
762 from: http://www.ncbi.nlm.nih.gov/pubmed/18653886
763 45. Vastenhouw NL, Brunschwig K, Okihara KL, Müller F, Tijsterman M, Plasterk
764 RHA. Gene expression: long-term gene silencing by RNAi. Nature [Internet]. 2006
765 Aug 24 [cited 2017 Jun 26];442(7105):882. Available from:
766 http://www.ncbi.nlm.nih.gov/pubmed/16929289
767 46. Pak J, Fire A. Distinct populations of primary and secondary effectors during RNAi
768 in C. elegans. Science [Internet]. 2007 Jan 12 [cited 2017 Jun 26];315(5809):241–
769 4. Available from: http://www.ncbi.nlm.nih.gov/pubmed/17124291
770 47. Guang S, Bochner AF, Burkhart KB, Burton N, Pavelec DM, Kennedy S. Small
771 regulatory RNAs inhibit RNA polymerase II during the elongation phase of
772 transcription. Nature [Internet]. 2010 Jun 13 [cited 2018 Feb 12];465(7301):1097–
773 101. Available from: http://www.ncbi.nlm.nih.gov/pubmed/20543824
774 48. Wedeles CJ, Wu MZ, Claycomb JM. Protection of germline gene expression by
775 the C. elegans Argonaute CSR-1. Dev Cell [Internet]. 2013 Dec 23 [cited 2017
776 Jun 29];27(6):664–71. Available from:
777 http://www.ncbi.nlm.nih.gov/pubmed/24360783
778 49. Conine CC, Moresco JJ, Gu W, Shirayama M, Conte D, Yates JR, et al.
779 Argonautes Promote Male Fertility and Provide a Paternal Memory of Germline
780 Gene Expression in C. elegans. Cell [Internet]. 2013 Dec [cited 2015 Jun
781 30];155(7):1532–44. Available from:
782 http://www.sciencedirect.com/science/article/pii/S0092867413014839
783 50. Seth M, Shirayama M, Gu W, Ishidate T, Conte D, Mello CC. The C. elegans
784 CSR-1 argonaute pathway counteracts epigenetic silencing to promote germline
785 gene expression. Dev Cell [Internet]. 2013 Dec 23 [cited 2015 Nov 11];27(6):656–
786 63. Available from: http://www.ncbi.nlm.nih.gov/pubmed/24360782
787 51. Gandhi SG, Bag I, Sengupta S, Pal-Bhadra M, Bhadra U. Drosophila oncogene
788 Gas41 is an RNA interference modulator that intersects heterochromatin and the
789 small interfering RNA pathway. FEBS J [Internet]. 2015 Jan [cited 2018 Jan
790 14];282(1):153–73. Available from:

bioRxiv preprint doi: https://doi.org/10.1101/273722; this version posted March 1, 2018. The copyright holder for this preprint (which was not certified by peer review) is the author/funder. All rights reserved. No reuse allowed without permission.

791 http://www.ncbi.nlm.nih.gov/pubmed/25323651
792 52. Pal-Bhadra M, Leibovitch BA, Gandhi SG, Chikka MR, Rao M, Bhadra U, et al.
793 Heterochromatic Silencing and HP1 Localization in Drosophila Are Dependent on
794 the RNAi Machinery. Science (80-) [Internet]. 2004 Jan 30 [cited 2018 Jan
795 14];303(5658):669–72. Available from:
796 http://www.ncbi.nlm.nih.gov/pubmed/14752161
797 53. Chang C-R, Wu C-S, Hom Y, Gartenberg MR. Targeting of cohesin by
798 transcriptionally silent chromatin. Genes Dev [Internet]. 2005 Dec 15 [cited 2018
799 Feb 27];19(24):3031–42. Available from:
800 http://www.ncbi.nlm.nih.gov/pubmed/16319193
801 54. Stein P, Rozhkov N V., Li F, Cárdenas FL, Davydenk O, Vandivier LE, et al.
802 Essential Role for Endogenous siRNAs during Meiosis in Mouse Oocytes. Cohen
803 PE, editor. PLOS Genet [Internet]. 2015 Feb 19 [cited 2018 Feb
804 4];11(2):e1005013. Available from:
805 http://www.ncbi.nlm.nih.gov/pubmed/25695507
806 55. Ortogero N, Schuster AS, Oliver DK, Riordan CR, Hong AS, Hennig GW, et al. A
807 Novel Class of Somatic Small RNAs Similar to Germ Cell Pachytene PIWI-
808 interacting Small RNAs. J Biol Chem [Internet]. 2014 Nov 21 [cited 2018 Feb
809 4];289(47):32824–34. Available from:
810 http://www.ncbi.nlm.nih.gov/pubmed/25320077
811 56. Li H, Durbin R. Fast and accurate short read alignment with Burrows-Wheeler
812 transform. Bioinformatics [Internet]. 2009 Jul 15 [cited 2018 Feb 11];25(14):1754–
813 60. Available from: http://www.ncbi.nlm.nih.gov/pubmed/19451168
814 57. Li H, Handsaker B, Wysoker A, Fennell T, Ruan J, Homer N, et al. The Sequence
815 Alignment/Map format and SAMtools. Bioinformatics [Internet]. 2009 Aug 15 [cited
816 2018 Feb 11];25(16):2078–9. Available from:
817 http://www.ncbi.nlm.nih.gov/pubmed/19505943
818 58. Langmead B, Trapnell C, Pop M, Salzberg SL. Ultrafast and memory-efficient
819 alignment of short DNA sequences to the human genome. Genome Biol [Internet].
820 2009 Mar 4 [cited 2018 Feb 19];10(3):R25. Available from:
821 http://genomebiology.biomedcentral.com/articles/10.1186/gb-2009-10-3-r25
822 59. Frøkjær-Jensen C, Wayne Davis M, Hopkins CE, Newman BJ, Thummel JM,
823 Olesen S-P, et al. Single-copy insertion of transgenes in Caenorhabditis elegans.
824 Nat Genet [Internet]. 2008 Nov 26 [cited 2018 Feb 11];40(11):1375–83. Available
825 from: http://www.ncbi.nlm.nih.gov/pubmed/18953339
826 60. R Core Team. R: A language and environment for statistical computing
827 [Internet]. R Foundation for Statistical Computing. Vienna, Austria; 2013.
828 Available from: http://www.r-project.org/
829

830
831

832

833

bioRxiv preprint doi: https://doi.org/10.1101/273722; this version posted March 1, 2018. The copyright holder for this preprint (which was not certified by peer review) is the author/funder. All rights reserved. No reuse allowed without permission.

834 **Figure Legends**

835 **Figure 1: A hypomorphic mutation in *gsp-2* results in transgenerational sterility**
836 **phenotype. (A)** Incidence of males in *gsp-2(yp14)* was 3.9% at 20°C and increased to
837 16.8% at 25°C. **(B)** Progeny of *gsp-2(yp14)* animals grown at 20°C 25°C were 6% and
838 41% Embryonic Lethal, respectively, compared to 97% of *gsp-2(tm301)* progeny
839 (N=20). **(C-D)** *gsp-2(yp14)* was identified to have a G to A mutation in exon 5 by whole
840 genome sequencing. This results in a D to N amino acid substitution in a well conserved
841 region of GSP-2. **(E)** When passaged at 20˚C for many generations N2, *gsp-2(yp14)*,
842 *lab-1* and *lab-1; gsp-2(yp14)* did not exhibit a loss of transgenerational fertility. **(F)** *gsp-*
843 *2(yp14)* and *lab-1* both exhibited loss of fertility at 25˚C and were completely sterile by
844 generation F17 and F11 respectively. A double mutant of *lab-1;gsp-2* went sterile
845 slightly faster than the individual single mutants and were completely sterile by F10.
846 (N≥40) **(G)** Analysis of incidence of males showed no jackpots of males at in *gsp-*
847 *2(yp14)* animals. *P<.0001 by T-test.
848

849 **Figure 2: Germline defects occur in *gsp-2* and temperature-sensitive small RNA**
850 **mutants at sterility. (A-E)** Representative images of DAPI stained germlines passaged
851 at 25°C. Germlines of either L4 (A) or adult control and sterile mutant animals were
852 stained, and the germline size quantified as either normal (B), short (C), atrophied (D) or
853 empty (E). **(H)** Germlines from *gsp-2(yp14)*, *lab-1*, *rsd-6*, *nrde-2* and *hrde-1* mutants
854 were examined and found have mostly normal morphology at the L4 stage but exhibited
855 germline atrophy in adult animals (N≥98). **(F,G,I)** In addition to germline atrophy, *gsp-*
856 *2(yp14)* animals displayed greater than the wildtype number of 6 DAPI bodies in

bioRxiv preprint doi: https://doi.org/10.1101/273722; this version posted March 1, 2018. The copyright holder for this preprint (which was not certified by peer review) is the author/funder. All rights reserved. No reuse allowed without permission.

857 oocytes at the generation at sterility in 32% of oocytes (N≥100). **(J)** 100% of adult *gsp-*
858 *2(tm301)* animals displayed normal germline size by DAPI staining (N=30). P-values
859 present in Table S2 and S3. Scale bar= 10um.
860
861 **Figure 3: Repetitive regions in the genome are desilenced in *gsp-2(yp14)* animals.**
862 **(A-F)** Confocal images of Cy5-labeled RNA FISH probes (green) and DAPI-stained
863 nuclei (blue). **(A,C,E)** RNA FISH probes show expression of Ch V repeats in the
864 germlines of *gsp-2(yp14)* (C) and *rsd-6* (E) animals grown at 25°C and only embryonic
865 expression in wildtype controls (A). **(B,D,F)** Probes against CeRep59 repeats reveal
866 similar germline expression in *gsp-2(yp14)* (D) and *rsd-6* (F) animals and embryo-only
867 expression in wildtype controls (B). All images were taken under the same condition.
868 The germ line is outlined with white line. Scale bar= 30um
869
870 **Figure 4: Temperature-sensitive small RNAi mutants exhibited similar times to**
871 **sterility as *gsp-2(yp14)* at 25°C.** Germline mortality assays all performed at 25°C **(A)**
872 Both *gsp-2(yp14)* and *hrde-1* animals exhibit similar times to sterility while *gsp-*
873 *2(yp14);hrde-1* double mutants display a slightly decreased time to sterility. p< .001**(B)**
874 *gsp-2(yp14)*, *nrde-2* and *rsd-6;gsp-2(yp14)* animals all go sterile in a similar number of
875 generations. p=.06 **(C)** *gsp-2(yp14)* and *rsd-6* exhibit similar times to sterility while *gsp-*
876 *2(yp14);rsd-6* double mutants become sterile at a slightly earlier generation. p<
877 .001(N≥40). Significance was tested using a log rank test.
878
879 **Figure 5: Increased histone phosphorylation is present in *gsp-2(yp14)* oocytes.**

bioRxiv preprint doi: https://doi.org/10.1101/273722; this version posted March 1, 2018. The copyright holder for this preprint (which was not certified by peer review) is the author/funder. All rights reserved. No reuse allowed without permission.

880 **(A-F)** Day 2 late stage adults passaged at 25°C stained with an pH3S10 antibody (red)
881 and DAPI marking the DNA (green). All samples were prepared at the same time and
882 imaged using identical settings. **(A)** Wildtype control oocytes show low levels of H3S10p
883 on condensed chromosomes. **(B)** *gsp-2(yp14)* oocytes have increased levels of
884 H3S10p covering the entire chromosomes. **(C, F)** Both *lab-1* and *hrde-1* mutants also
885 display increased levels of H3S10p but *nrde-2* **(D)** and *rsd-6* **(E)** do not. (N≥20**) (G-L)**
886 Day 2 late generation or sterile adults passaged at 25°C stained with an pH3S10
887 antibody (red) and DAPI marking the DNA (green). All samples were prepared at the
888 same time and imaged using identical settings. **(G)** Control oocytes show low levels of
889 localized H3T3p on the short arms of the condensed chromosomes. **(H)** *gsp-2(yp14)*
890 oocytes contain high levels of H3T3p that are expanded to cover the entire condensed
891 chromosome. **(I-L)** *lab-1*, *hrde-1*, *rsd-6* and *nrde-2* all display varying levels of increased
892 H3T3p staining compared to wildtype controls but localization to the short arms is still
893 relatively normal. (N≥20) **(M)** Quantification of fluorescence intensity of H3S10p staining
894 in N2, *gsp-2(yp14)* animals grown at 20°C and 25°C, *rsd-6*, *nrde-2*, *hrde-1*, and *lab-1*
895 shows significant difference in staining intensity between N2 and mutants grown at the
896 same temperature (except for *nrde-2*) and between *gsp-2(yp14)* mutants grown at 20°C
897 and 25°C. (N≥20) **(N)** Quantification of fluorescence intensity of H3T3p staining in N2,
898 *gsp-2(yp14)* animals grown at 20°C and 25°C, *rsd-6*, *nrde-2*, *hrde-1*, and *lab-1* shows
899 significant difference in staining intensity between N2 and mutants grown at the same
900 temperature and between *gsp-2(yp14)* mutants grown at 20°C and 25°C. (N≥20) Scale
901 bar= 10um.
902

bioRxiv preprint doi: https://doi.org/10.1101/273722; this version posted March 1, 2018. The copyright holder for this preprint (which was not certified by peer review) is the author/funder. All rights reserved. No reuse allowed without permission.

903 **Figure 6: GSP-2 promotes multigenerational transgene silencing**

904 **(A)** *gsp-2(yp14)* mutants do not exhibit single generation RNAi defects while *rsd-6* and
905 *nrde-2* mutants are defective for single generation RNAi. **(B)** *cpIs12* remains
906 undetectable for multiple generations after RNAi treatment. However, in *gsp-*
907 *2(yp14);cpIs12* animals treated with RNAi cpIs12 only remains undetectable for one
908 generation and by generation 3 exhibit close to wildtype levels of expression. **(C)** When
909 LP138, a GFP transgene, is passaged as a heterozygote for multiple generations it is
910 silenced in the germline. LP138 passaged as a heterozygote in a *gsp-2(yp14)* mutants
911 results in only partial silencing over 5 generations suggesting defective heterozygous
912 transgene silencing. **(D)** Comparison of small RNAs in *rsd-6*, *gsp-2* and *spr-5* mutants
913 showing a great overlap in small RNA identity between *gsp-2* and *spr-5*. **(E)** Graph
914 showing levels of piRNA expression in N2 controls, *rsd-6*, *gsp-2* and *spr-5* mutants at
915 both early (E1) and late (L1) generations grown at 25°C.

916

917 **Figure 7: A model for the roles of GSP-2 and small RNA-mediated silencing in**
918 **promoting germline immortality.** We propose that both GSP-2 and small RNA-
919 mediated silencing regulation the transgenerational inheritance of the epigenome. When
920 these pathways are disrupted loss of epigenetic regulation can lead to germline atrophy.
921 **A)** GSP-2/LAB-1 promote homolog pairing at the initiation of meiosis between
922 homologous chromosomes during pachytene. **(A')** GSP-2/LAB-1 promote sister
923 chromatid cohesion during prophase. **B)** GSP-2 modulates small RNA silencing
924 machinery promoting small RNA silencing potentially through histone dephosphoryation
925 in a manner that promotes epigenetic silencing, **C)** Previous work has shown that PRG-
926 1 is important for heterozygous transgene silencing (red =active transgene and black

bioRxiv preprint doi: https://doi.org/10.1101/273722; this version posted March 1, 2018. The copyright holder for this preprint (which was not certified by peer review) is the author/funder. All rights reserved. No reuse allowed without permission.

927 =silenced) in a similar manner to GSP-2. GSP-2/LAB-1 could function to silence
928 heterozygous regions of DNA which disrupt meiotic pairing between homologs or
929 cohesion between sister chromatids.
930
931 **Supplemental Figure 1: Mapping and non-complementation test of *gsp-2(yp14)***
932 **(A)** Map of genomic region surrounding *gsp-2* on Chr. *III*. **(B)** Mapping of *gsp-2(yp14)*
933 between *dpy-17* and *unc-32* on Chr. *III* placing *yp14* at -1.08. **(C)** Non-complementation
934 test for Him phenotype between *gsp-2(yp14)* and *gsp-2(tm301)* showed an incidence of
935 males of 5.7% at 20°C.
936
937 **Supplemental Figure 2: Loss of cohesion did not cause germline atrophy**
938 DAPI staining and germline analysis showed no germline atrophy in *smc-3* and *coh-3;*
939 *coh-4* mutants and minor defects in *air-2* animals suggesting loss of chromosome
940 cohesion alone does not cause germline atrophy. (N=30)
941
942 **Supplemental Figure 3: *spr-5* and *gsp-2* show overlap in their small RNA**
943 **populations (A)** Multigenerational inheritance assay using a second transgene *pkls32*
944 in the background of *hrde-1* and *gsp-2* mutants. **(B-E)** Comparison of small RNAs in
945 *rsd-6*, *gsp-2* and *spr-5* mutants: **(B)** *rsd-6* vs *gsp-2*, **(C)** *spr-5* vs *gsp-2*, **(D)** *rsd-6* vs *spr-*
946 *5* and **(E)** N2 vs *gsp-2*.
947
948
949

bioRxiv preprint doi: https://doi.org/10.1101/273722; this version posted March 1, 2018. The copyright holder for this preprint (which was not certified by peer review) is the author/funder. All rights reserved. No reuse allowed without permission.

950
951
952

	Males	Exp Dead Emb	Exp Live Worms	Obs Dead Emb	Obs Live Worms	p-value
20°C gsp-2(yp14)	164	820	5290	88	1492	<0.0001
25°C gsp-2(yp14)	155	775	964	481	1380	<0.0001

953
954

955 **Supplemental Table 1: Expected vs Observed Embryonic Lethality**

956
957
958
959
960
961

bioRxiv preprint doi: https://doi.org/10.1101/273722; this version posted March 1, 2018. The copyright holder for this preprint (which was not certified by peer review) is the author/funder. All rights reserved. No reuse allowed without permission.

962

963

	N2	*gsp-2(yp14)*	*lab-1*	*gsp-2(tm301)*	*rsd-6*	*nrde-2*	*hrde-1*	*smc-3*	*coh-3/4*	*air-2*
N2	1	1.008E-85	1.5E-90	1	2E-85	1.3E-67	2E-59	1	1	8.1E-55
gsp-2(yp14)	1E-85	1	5.1E-17	1.646E-45	8E-06	1.4E-06	0.0154	1.2E-40	6.7E-41	5.4E-23
lab-1	2E-90	5.13E-17	1	2.2041E-47	5E-11	1.2E-16	8E-17	7.3E-43	4.4E-43	1.8E-19
gsp-2(tm301)	1	1.646E-45	2.2E-47	1	1E-43	8.2E-32	9E-27	1	1	8.2E-25
rsd-6	2E-85	7.718E-06	4.9E-11	1.3493E-43	1	3.4E-12	9E-11	4E-39	2.5E-39	3.5E-29
nrde-2	1E-67	1.383E-06	1.2E-16	8.175E-32	3E-12	1	0.248	7.5E-28	4.9E-28	8.4E-08
hrde-1	2E-59	0.01536	7.8E-17	9.4732E-27	9E-11	0.248	1	4.1E-23	2.7E-23	7.6E-10
smc-3	1	1.151E-40	7.3E-43	1	4E-39	7.5E-28	4E-23	1	1	1.9E-21
coh-3/4	1	6.658E-41	4.4E-43	1	2E-39	4.9E-28	3E-23	1	1	1.3E-21
air-2	8E-55	5.438E-23	1.8E-19	8.1847E-25	4E-29	8.4E-08	8E-10	1.9E-21	1.3E-21	1

964

965 **Supplemental Table 2: P-values for adult germline defects in *gsp-2* and**

966 **temperature-sensitive small RNA mutants**

967

bioRxiv preprint doi: https://doi.org/10.1101/273722; this version posted March 1, 2018. The copyright holder for this preprint (which was not certified by peer review) is the author/funder. All rights reserved. No reuse allowed without permission.

968

969

970

	N2	gsp-2(yp14)	lab-1	gsp-2(tm301)	rsd-6	nrde-2	hrde-1
N2	1	2.23E-05	0.036	1	1	0.0031	0.005
gsp-2(yp14)	2.23E-05	1	1	0.00140304	4E-04	1	1
lab-1	0.036421	1	1	0.69600428	0.126	1	1
gsp-2(tm301)	1	0.001403	0.696	1	1	0.0859	0.119
rsd-6	1	0.0003621	0.126	1	1	0.0172	0.024
nrde-2	0.003076	1	1	0.08591014	0.017	1	1
hrde-1	0.00461	1	1	0.11911645	0.024	1	1

971 **Supplemental Table 3: P-values for L4 germline defects in *gsp-2* and temperature-**

972 **sensitive small RNA mutants**

973

Figure 1

bioRxiv preprint doi: https://doi.org/10.1101/273722; this version posted March 1, 2018. The copyright holder for this preprint (which was not certified by peer review) is the author/funder. All rights reserved. No reuse allowed without permission.

Click here to download Figure Fig1.1.tif

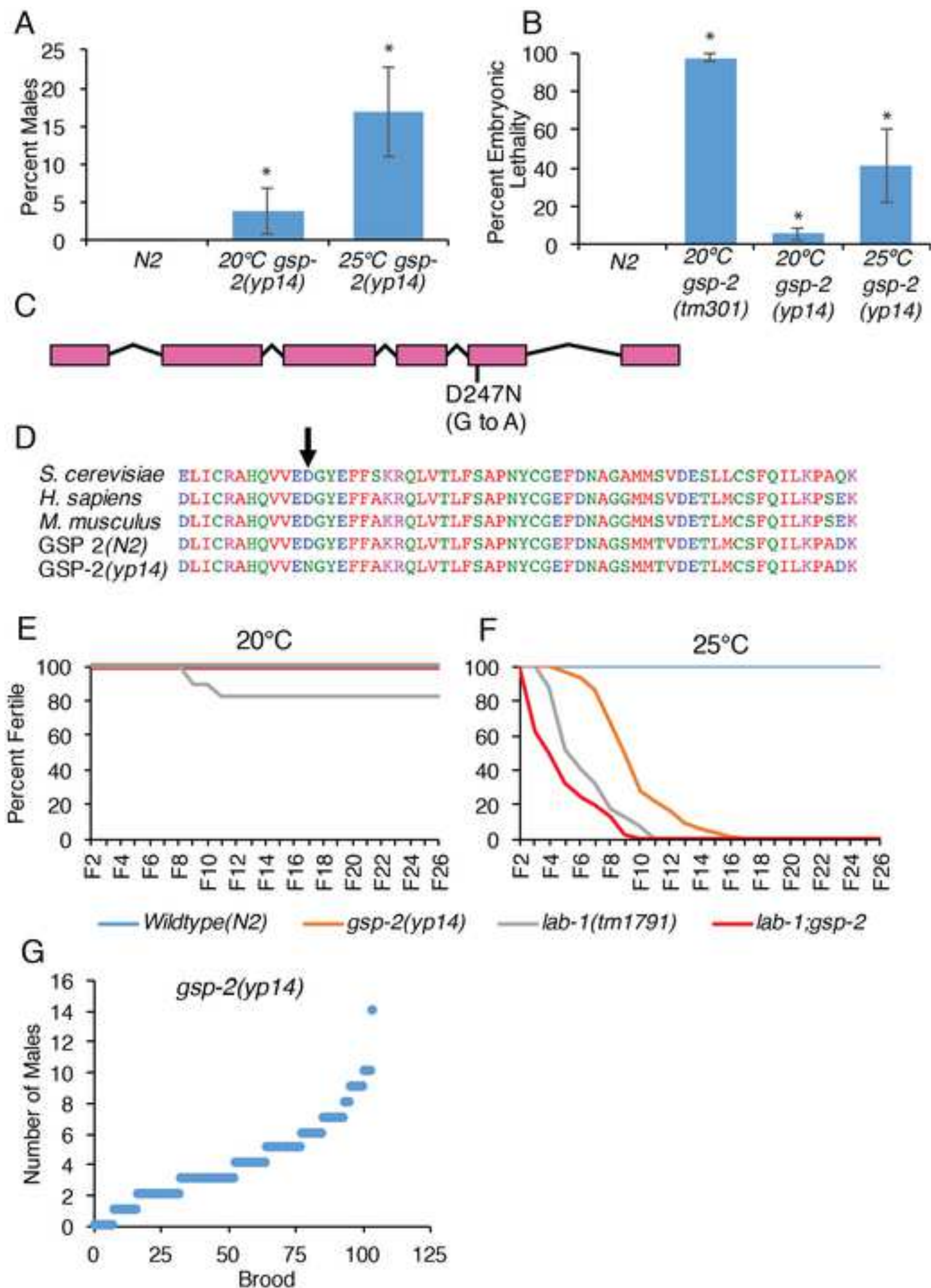

Figure 2

Click here to download Figure Fig2.1.tif

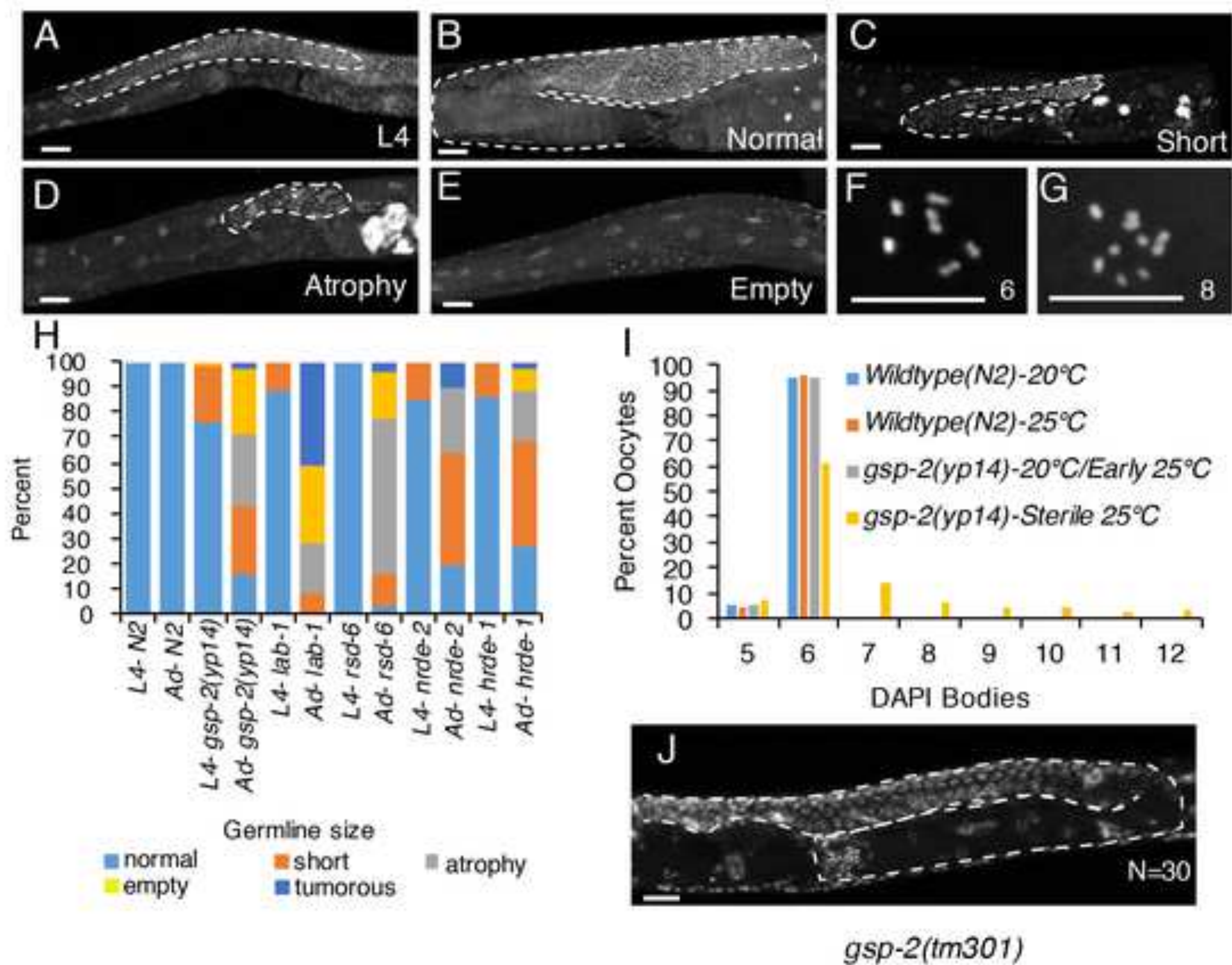

bioRxiv preprint doi: https://doi.org/10.1101/273722; this version posted March 1, 2018. The copyright holder for this preprint (which was not certified by peer review) is the author/funder. All rights reserved. No reuse allowed without permission.

Figure 3

Click here to download Figure fig3.1.tif

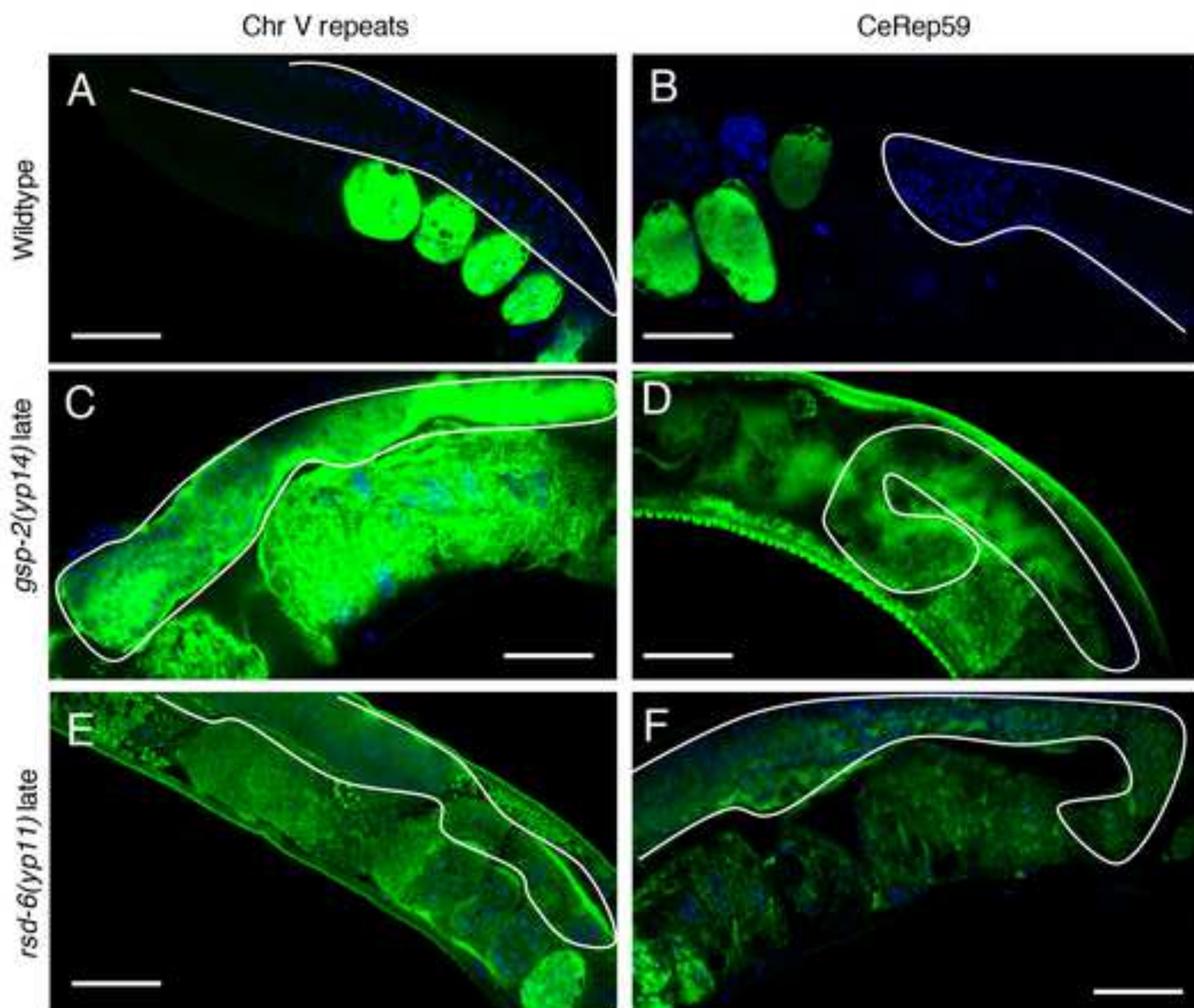

bioRxiv preprint doi: https://doi.org/10.1101/273722; this version posted March 1, 2018. The copyright holder for this preprint (which was not certified by peer review) is the author/funder. All rights reserved. No reuse allowed without permission.

Figure 4

bioRxiv preprint doi: https://doi.org/10.1101/273722; this version posted March 1, 2018. The copyright holder for this preprint (which was not certified by peer review) is the author/funder. All rights reserved. No reuse allowed without permission.

Click here to download Figure fig4.1.tif

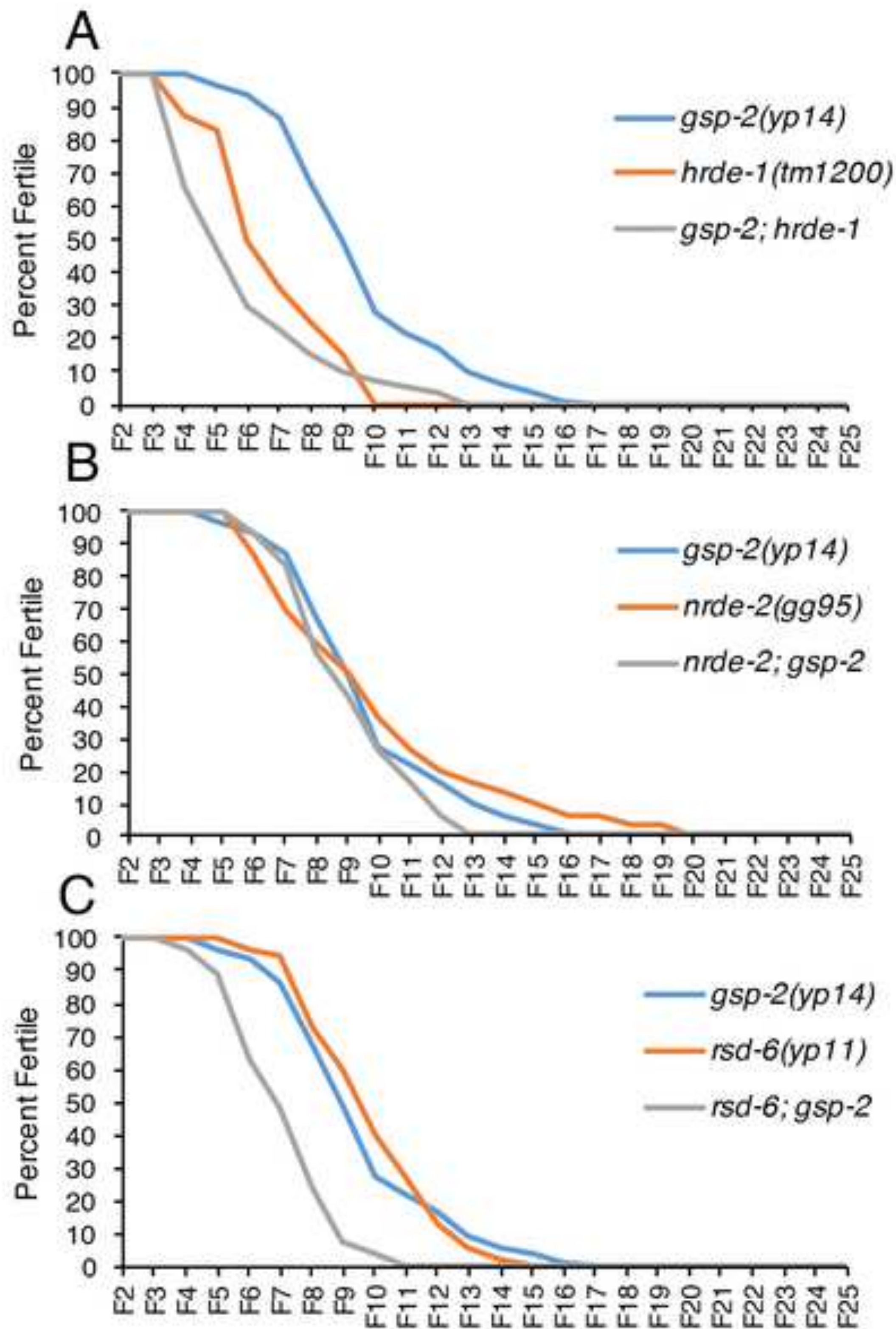

Figure 5

bioRxiv preprint doi: https://doi.org/10.1101/273722; this version posted March 1, 2018. The copyright holder for this preprint (which was not certified by peer review) is the author/funder. All rights reserved. No reuse allowed without permission.

Click here to download Figure fig5.1.tif

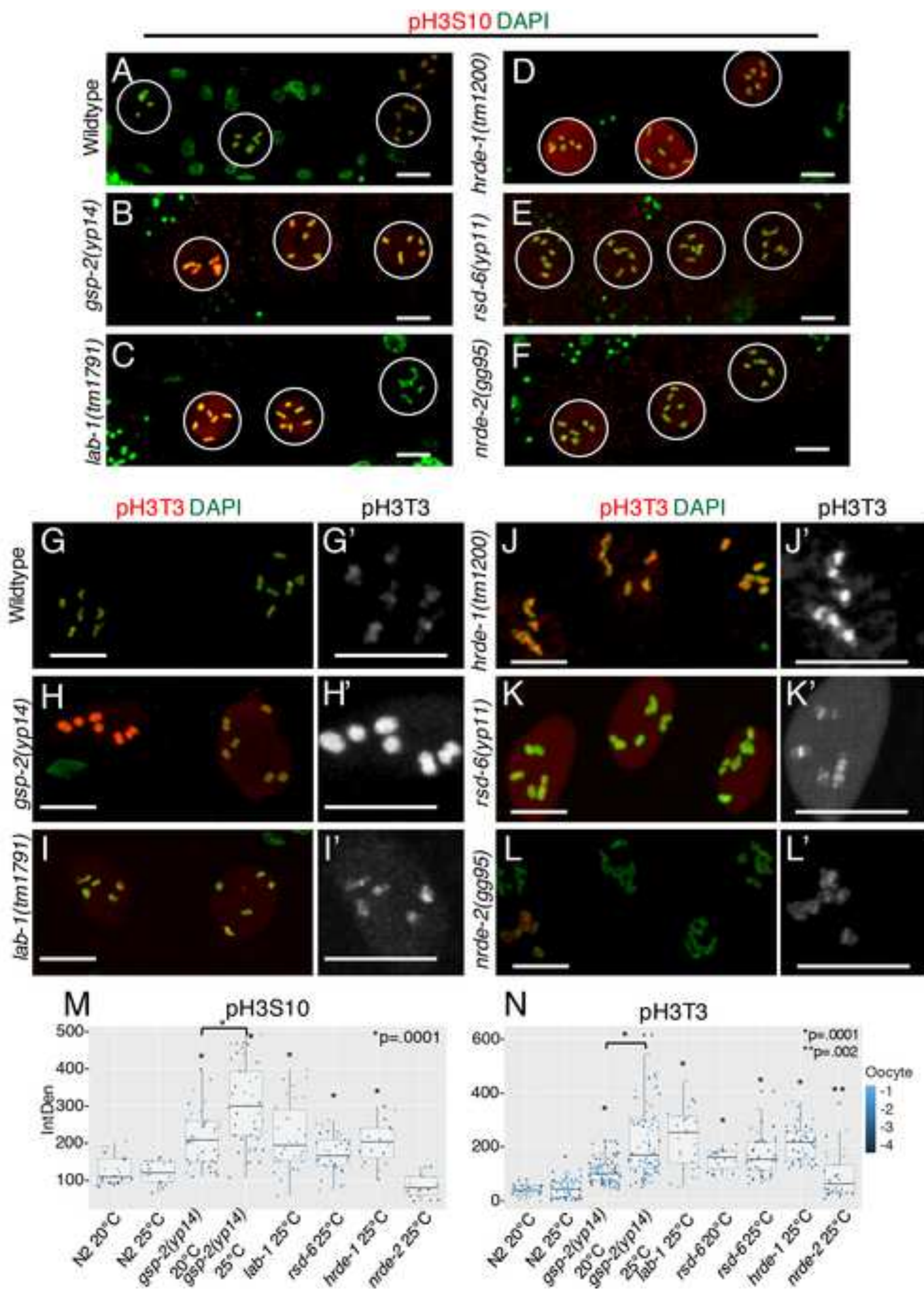

Figure 6 bioRxiv preprint doi: https://doi.org/10.1101/273722; this version posted March 1, 2018. The copyright holder for this preprint (which was not certified by peer review) is the author/funder. All rights reserved. No reuse allowed without permission. Click here to download Figure Fig6.1.tif

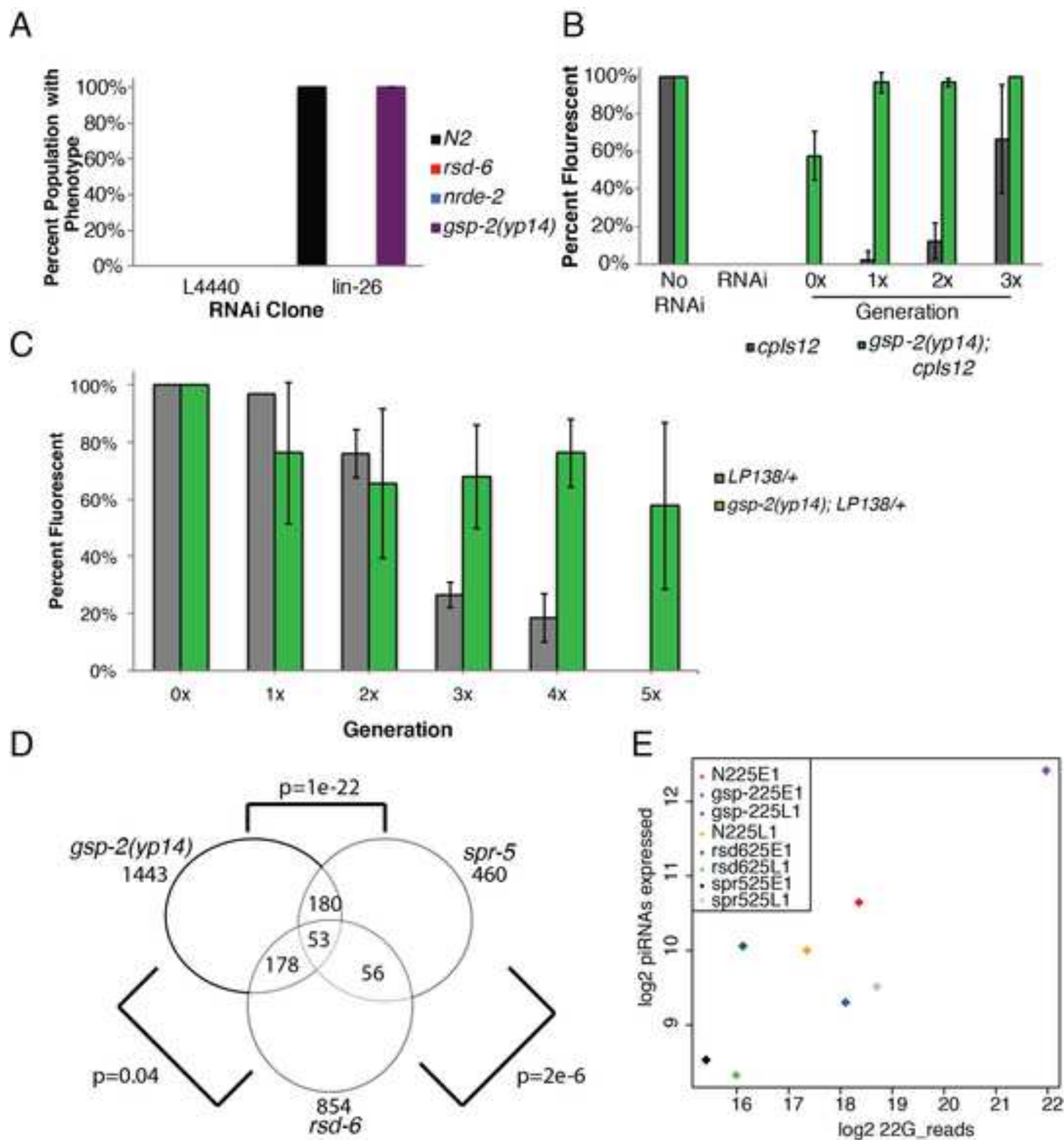

Figure 7 Click here to download Figure FIg7.1.tif

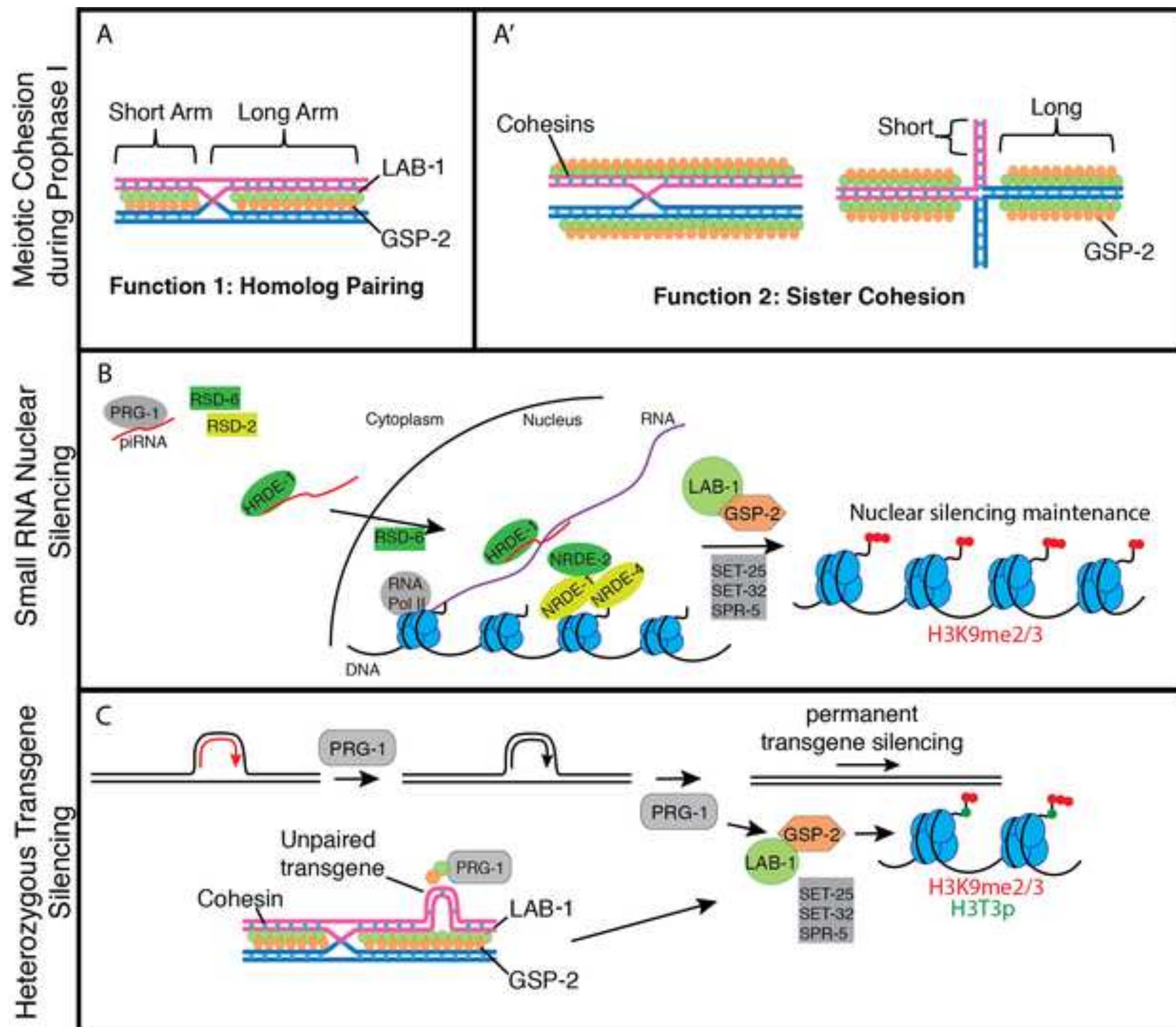

bioRxiv preprint doi: https://doi.org/10.1101/273722; this version posted March 1, 2018. The copyright holder for this preprint (which was not certified by peer review) is the author/funder. All rights reserved. No reuse allowed without permission.